

Sterile Neutrinos in Big Bang Nucleosynthesis

Diplomarbeit
von
Robert Buras

München, Dezember 1999

Physik-Department der Technischen Universität München
Institut für Theoretische Physik T39
Prof. Dr. Wolfram Weise
Ausgefertigt am Max-Planck-Institut für Physik
(Werner-Heisenberg-Institut)
bei Dr. Georg Raffelt

Zusammenfassung

Neutrinoophysik hat in diesem Jahrzehnt sehr an Popularität gewonnen, nicht zuletzt aufgrund der Messung von Neutrinooszillationen. Allerdings lassen sich nicht gleichzeitig alle Oszillationsexperimente vollständig durch das mit Neutrinomassen erweiterte Standardmodell erklären. Eine mögliche Lösung bietet die Einführung eines vierten Neutrinos, das jedoch aufgrund der Z^0 Resonanzbreite nicht schwach wechselwirken darf.

Ein solches steriles Neutrino könnte aufgrund seiner gravitativen Wechselwirkung sowie der Neutrinooszillationen einen Einfluß auf die primordiale Nukleosynthese haben. Dieses Phänomen ist schon in einer Vielzahl von Veröffentlichungen behandelt worden. Es hat sich jedoch als sehr schwierig herausgestellt, das nicht-lineare Differentialgleichungssystem, daß die Neutrinooszillationen im frühen Universum beschreibt, zu lösen.

Während bisherige Publikationen sich meistens auf numerische Rechnungen beschränkten, untersuchen wir das System analytisch, wobei wir als einzige Näherung die Impulsverteilung vernachlässigen. Dabei achten wir besonders auf das Verhalten des Systems kurz nachdem die Resonanztemperatur unterschritten worden ist. Im Einklang mit anderen Publikationen sehen wir einen exponentiellen Anstieg in der Neutrinoasymmetrie. Wir beweisen, daß für einen signifikanten Bereich der Mischungsparameter δm^2 und $\sin^2 2\theta$ diese Neutrinoasymmetrie zu oszillieren beginnt und sogar das Vorzeichen wechselt. Damit werden numerische Kalkulationen bestätigt, die diesen Effekt schon früher entdeckt haben, deren numerische Stabilität jedoch angezweifelt wurde.

Acknowledgement

I would especially like to thank my supervisor Georg Raffelt, who introduced me to this exciting subject and helped me prepare for a life as a physicist.

I would also like to thank Wolfram Weise for his willing support, and for teaching me quantum mechanics.

Thanx to Klaus Böcker for listening to all my crazy ideas, and to Björn Pötter for his computer guidance.

Extra thanx to Mr. Hiermeier who never gave up showing me the fun in Mathematics. Peace to everybody else who should be standing here, I'd never be finished.

Contents

1	Introduction	3
2	Big Bang Nucleosynthesis	8
2.1	Dynamics in the Radiation Epoch	8
2.2	Number Densities and Fermion Asymmetries	10
2.3	Helium Abundance	11
2.4	Non-Standard Neutrinos	13
2.5	Observational Results	14
2.6	Summary	15
3	Neutrino Oscillations	16
3.1	Equation of Motion	16
3.2	Medium Effects	18
3.3	Density Matrix Formalism for Two-Flavor Oscillations	20
3.4	Scattering Processes	21
4	Oscillating Lepton Asymmetry	23
4.1	Simplified Model	23
4.2	Numerical Solution	26
4.3	Spherical Coordinates	28
4.4	Initial Conditions	31
4.5	Quasi-Static Solutions	31
4.6	Evolution Towards the Resonance	34
4.7	Evolution at Resonance	36
4.7.1	Static Approximation after Resonance	36
4.7.2	Mathematical Pendulum	37

4.7.3	The Factor \mathbf{g}	41
4.7.4	Proof for Oscillations	44
5	Conclusions	46
A	Quasi-Static Approximation and its Range of Validity	48

Chapter 1

Introduction

Neutrino physics has become very popular during the past decade. The main impetus in this field has come from the strong improvements in detecting neutrinos; there is now strong evidence from two natural neutrino sources, the solar core [1] and the Earth's atmosphere [2], that neutrinos of a certain flavor disappear on their way to the detector. Furthermore, a neutrino beam produced in the laboratory has been found to change flavor in the LSND experiment [3].

The most natural explanation for these anomalies is achieved by extending the Standard Model with neutrino masses. Together with the Cabibbo-Kobayashi-Maskawa (CKM) matrix for the lepton sector, the masses imply flavor mixing; neutrino oscillations have been born [4]. Such oscillations can be fully parameterized by the differences between the squared masses $\delta m_{ij}^2 \equiv m_j^2 - m_i^2$ and the mixing angles θ_{ij} . Also, a possible phase in the CKM matrix could induce CP violation. With these neutrino oscillations, the experiments can be explained by the solutions presented in Table 1.1.

However, with this straightforward extension of the Standard Model it is not possible to explain all three experiments simultaneously, simply because the trivial condition

$$\sum \delta m_{ij}^2 = (m_3^2 - m_2^2) + (m_2^2 - m_1^2) + (m_1^2 - m_3^2) = 0 \quad (1.1)$$

cannot be fulfilled by the data. Hence, many interesting new models have been suggested to explain the three different experiments. One of the most appealing possibilities is the existence of a fourth neutrino. Since the Z^0 decay width [6] excludes more than three standard neutrinos, this new flavor must be inert with respect to the standard weak interaction.

Experiment	Favored Channel	$ \delta m^2 [\text{eV}^2]$	$\sin^2 2\theta$
Solar			
Vacuum	$\nu_e \rightarrow \text{anything}$	$(0.5-8) \times 10^{-10}$	0.5-1
MSW (small angle)	$\nu_e \rightarrow \text{anything}$	$(0.4-1) \times 10^{-5}$	$10^{-3}-10^{-2}$
MSW (large angle)	$\nu_e \rightarrow \nu_\mu$ or ν_τ	$(3-30) \times 10^{-5}$	0.6-1
Atmospheric	$\nu_\mu \rightarrow \nu_\tau$	$(1-8) \times 10^{-3}$	0.85-1
	$\nu_\mu \rightarrow \nu_s$	$(2-7) \times 10^{-3}$	0.85-1
LSND	$\bar{\nu}_\mu \rightarrow \bar{\nu}_e$	0.2-10	$(0.2-3) \times 10^{-2}$

Table 1.1: *Results from neutrino oscillation experiments [5]. The values are nominal 2σ ranges.*

Although the hypothesis of such a sterile neutrino may seem highly speculative, its possible existence is the most far-reaching implication of the current experimental situation. It is certainly worthwhile to investigate its consequences! Sterile neutrinos would have a strong impact on certain astrophysical environments due to their mixing with active neutrinos. These effects would become especially important under extreme conditions, like in core-collapse supernovae [7] and in the Early Universe.

It is the impact of sterile neutrinos in the Early Universe, and in particular the outcome of the primordial nucleosynthesis, that has been the subject of an intense recent debate. By incorporating sterile neutrinos into the well understood mechanism of standard Big Bang nucleosynthesis (BBN), two frontiers of physics would be connected in one phenomenon, making this a powerful tool for predictions.

The production of primordial nuclei depends sensitively on the expansion rate of the Universe, which in turn depends on the number density of sterile neutrinos. This simple correlation is well known [8]; the actual challenge is to deduce how much the sterile neutrino sector is populated. Since the only connection between sterile neutrinos and ordinary matter, apart from gravity, is given by oscillations, this phenomenon must be the key for creating a relation between sterile neutrino parameters and Big Bang nucleosynthesis predictions.

In the beginning of the 1990's, the number density for sterile neutrinos at the time of primordial nucleosynthesis was calculated depending on the

parameters for oscillations between an active and a sterile neutrino, δm^2 and θ [9, 10]. The idea was to constrain the allowed parameter space, since strong observational results (which have weakened since) set an upper bound on the number density of the ν_s . In these calculations, the influence of the thermal plasma on the mixing parameters was included, but the small CP asymmetric contributions were neglected. The constraints were so strong that they clearly excluded the $\nu_\mu \leftrightarrow \nu_s$ solution for the atmospheric neutrino anomaly.

In 1995, Foot, Thomson and Volkas [11] found an interesting effect by including the CP asymmetric contributions; the asymmetry could induce different population rates for the sterile neutrinos and antineutrinos, or equivalently, different depopulation rates for the active neutrinos and antineutrinos. This would change the neutrino asymmetry and thus would have an influence on the population rates. They found that this back-reaction could amplify an initially small CP asymmetry by several orders of magnitude for a large range of parameter space. (Actually, this back-reaction had been discussed much earlier by Barbieri and Dolgov [10], but they erroneously found the effect to be small.)

The implications from this new effect were manifold. The most interesting conclusion was given by a model in which $\nu_\tau \leftrightarrow \nu_s$ oscillations created a large ν_τ asymmetry, which in turn suppressed $\nu_\mu \leftrightarrow \nu_s$ oscillations [12–17]. In such a model, the atmospheric neutrino anomaly could be explained by $\nu_\mu \leftrightarrow \nu_s$ oscillations without the sterile neutrinos coming into thermal equilibrium. Another thoroughly discussed implication treated the impact of a large ν_e asymmetry on primordial nucleosynthesis [13, 18, 19]; the large chemical potential μ_e would change the neutron-to-proton ratio and thus the nuclear abundances.

Clearly, sterile neutrinos can only be included correctly into BBN if the mechanism producing large neutrino asymmetries is revealed. Unfortunately, this has proven to be a very difficult task. A series of papers have been published on this subject by several groups [12–36], but the situation remains unclear. The main problem is that the system of differential equations describing the mixing is very complex: one has to treat neutrinos of different momentum separately, and one especially has to take care of the non-linear terms in the equations. Therefore, most works tried to solve the problem with numerical calculations. Thereby, they often used either the adiabatic approximation, which simplifies the equations for a given momentum, or they neglected the momentum distribution. Only during the past year some au-

thors claim to have solved the full system of differential equations numerically [14, 15, 20].

Due to these difficulties in solving the system, the different works present contradictory solutions: when neglecting the momentum distribution, the neutrino asymmetry shows an oscillating behavior [21, 22]. The system then ends up with a calculable value of the ν asymmetry, but with unpredictable sign. Such a scenario would introduce domains in the Early Universe with different signs of neutrino asymmetry [23]. On the other hand, applying the adiabatic approximation [13] is questionable since the neutrino oscillations are not adiabatic close to the resonance for the parameter space of interest. Here the neutrino asymmetry does not oscillate. Since the numerical calculation using the full system of differential equations is very CPU-time consuming, one also has to question whether the calculations are done with sufficient accuracy and whether the numerics are stable at all. After all, non-linear systems tend to show chaotic behavior. Besides, different results achieved by these calculations are contradictory on the point of oscillating neutrino asymmetry [15, 23].

All these numerical works have in common that they predict a similar final absolute neutrino asymmetry (if effects of neutrino domains are ignored) of orders 10^{-2} –1. But even this outcome has been questioned very recently in an analytical work by Dolgov *et al.* [24], who end up with a final asymmetry several orders of magnitude lower than the former results. Thus, the only point on which all works agree is that oscillations between sterile and active neutrinos in the Early Universe have the potential of creating a neutrino asymmetry at least of order 10^{-5} , a number which is still large compared to the baryon asymmetry, $\eta = \mathcal{O}(10^{-9})$.

The main problem is to get a grip on the exact behavior of the non-linear system. Our work will try to bring some clarity into this subject. Most of the former papers were strongly based on numerical calculations. In this paper, the discussion will be based on a thorough analytical treatment, which will be supported by simple numerical calculations. We will describe the evolution of the system, neglecting the momentum distribution, and compare our results with a numerical solution for the parameters $(\delta m^2, \sin 2\theta_0) = (-1 \text{ eV}^2, 10^{-4})$. It should be the job of future investigations to include the effects from the momentum distribution.

In Chapter 2, those aspects of the Early Universe and Big Bang nucleosynthesis will be summarized which are important for our system. Chapter 3 contains all relevant information about neutrino oscillations in matter. In

Chapter 4, we analyze the system in the simple two flavor case. After introducing initial conditions, we prove that our system creates oscillations of the lepton asymmetry. In Chapter 5, we summarize our findings.

Chapter 2

Big Bang Nucleosynthesis

We study the influence of neutrinos, in particular their effective number of flavors and the ν_e chemical potential, on Big Bang nucleosynthesis (BBN). To this end we first describe the expansion of the Early Universe before and during BBN. We define number density and lepton asymmetry. Next, we give a short summary of BBN, concentrating on the main product, ${}^4\text{He}$, and we estimate the influence the neutrino sector can have on its abundance. Finally, we summarize the observational results.

2.1 Dynamics in the Radiation Epoch

In order to discuss the influence of neutrinos on BBN we need to introduce some general concepts pertaining to the relevant cosmological epoch. Naturally, we only need to look at the Universe at times before and during BBN, i.e. at temperatures above 0.1 MeV. On the other hand, for the mixing parameters we will consider, neutrino oscillations are strongly damped at temperatures much higher than the QCD phase transition scale Λ_{QCD} of around 200 MeV. The temperatures of interest are therefore between 200 MeV and 0.1 MeV, corresponding to cosmological time scales from 10^{-5} s to 3 min.

The Universe during this epoch is flat, homogeneous and isotropic, and can therefore be described by the Robertson-Walker metric. The Friedmann equation for these conditions is simply [8]

$$H^2(t) = \frac{8\pi G}{3} \rho(t), \quad (2.1)$$

where $H(t) = \dot{R}(t)/R(t)$ is the Hubble parameter or expansion rate, R the

cosmic scale factor, $G = m_{\text{pl}}^{-2}$ Newton's constant, and $m_{\text{pl}} = 1.22 \times 10^{19}$ GeV the Planck mass. Because the energy density ρ is dominated by radiation, it scales as R^{-4} , which upon integrating (2.1) gives $H = \frac{1}{2} t^{-1}$.

The radiation density is usually expressed in the form

$$\rho = \frac{\pi^2}{30} g_* T^4, \quad (2.2)$$

where T is the photon temperature and g_* the total effective number of relativistic degrees of freedom,

$$g_* = \sum_{i=\text{bosons}} g_i \left(\frac{T_i}{T}\right)^4 + \frac{7}{8} \sum_{i=\text{fermions}} g_i \left(\frac{T_i}{T}\right)^4. \quad (2.3)$$

Here, g_i is the number of internal degrees of freedom of particle species i and T_i is its temperature. If we insert (2.2) into (2.1) and use $t = 1/2H$, we finally derive a relationship between time and temperature:

$$t = \frac{1}{2} \sqrt{\frac{90}{8\pi^3}} g_*^{-1/2} \frac{m_{\text{pl}}}{T^2} = 0.301 g_*^{-1/2} \frac{m_{\text{pl}}}{T^2}. \quad (2.4)$$

As another consequence, we note that $T \propto R^{-1}$ as long as $g_* = \text{const}$.

In the range $1 \text{ MeV} \lesssim T \lesssim 100 \text{ MeV}$, the only particles which contribute significantly to the radiation density are photons ($g_\gamma = 2$), electrons and positrons ($g_e = 4$), and three left-handed neutrino families with $g_\nu = 2$ each. For all of them $T_i = T$ applies as long as they remain in thermal equilibrium so that $g_* = 10.75$. Any additional neutrino species would add another $7/8$ per internal degree of freedom. For $T \gtrsim 100 \text{ MeV}$, g_* is higher due to the presence of muons and pions, and for $T \gtrsim \Lambda_{\text{QCD}} \approx 200 \text{ MeV}$ many gluon and quark degrees of freedom are excited. For $T \lesssim 1 \text{ MeV}$, the electrons and positrons become non-relativistic and annihilate, reducing g_* by $(7/8)g_e = 7/2$. This effect heats the photons (the neutrinos are already decoupled) so that T_ν/T is reduced to $(4/11)^{1/3}$, leading to $g_* = 3.36$.

In our subsequent discussion we will ignore these effects and always use the value $g_* = 10.75$, implying

$$H = \frac{1}{2} t^{-1} = 5.5 \frac{T^2}{m_{\text{pl}}}. \quad (2.5)$$

This is a good approximation as long as the oscillation parameters are such that the crucial events happen in the range $1 \text{ MeV} \lesssim T \lesssim 100 \text{ MeV}$.

2.2 Number Densities and Fermion Asymmetries

Because we want to study the influence of neutrino number densities and matter-antimatter asymmetries, we introduce appropriate measures for them. It is convenient to normalize these quantities to the photon number density

$$n_\gamma = 2 \frac{\zeta_3}{\pi^2} T^3, \quad (2.6)$$

where ζ is the Riemann zeta function with $\zeta_3 \approx 1.202$.

Fermions may have non-vanishing chemical potentials μ_i which affect their number densities. In addition, a non-vanishing μ_i implies a CP asymmetry for species i which we parameterize as

$$A_i \equiv \frac{n_i - \bar{n}_i}{n_\gamma}, \quad (2.7)$$

where \bar{n}_i refers to the antiparticle density.

At temperatures below the QCD phase transition virtually no hadronic antimatter exists. Since there are no baryon-number violating interactions at this late epoch, the total baryon number is conserved. Therefore, the number density of baryons, n_B , scales as R^{-3} or T^3 . The baryon asymmetry

$$A_B = \frac{n_B - \bar{n}_B}{n_\gamma} \approx \frac{n_B}{n_\gamma} \quad (2.8)$$

is thus constant under the cosmic expansion.

The commonly used present-time baryon asymmetry η is related to our A_B through

$$\eta = \frac{4}{11} A_B = 1 \text{ to } 6 \times 10^{-10}. \quad (2.9)$$

The difference is due to photon heating when electrons and positrons annihilate, an effect which modifies all asymmetries. We will always take A_i to refer to the fermion asymmetry of species i at the epoch before e^+e^- annihilation.

For $T < \Lambda_{\text{QCD}}$, almost all baryons are either neutrons n or protons p , which implies that $n_B = n_n + n_p$. The non-trivial evolution of n_n and n_p will be discussed in the next section.

We will assume that the Universe is charge neutral. Neglecting muons and pions, we therefore use

$$A_e = A_p \quad (2.10)$$

for the electron asymmetry.

Turning to neutrinos, we can safely neglect their mass. Therefore, their number densities are given by

$$n_\nu = \int \frac{d^3\mathbf{p}}{(2\pi)^3} f(p, T, \mu), \quad (2.11)$$

where $E = p = |\mathbf{p}|$, $f(p, T, \mu) = [e^{(p-\mu)/T} + 1]^{-1}$ is the Fermi-Dirac phase-space distribution function, and μ is the chemical potential. For very small asymmetries ($\mu \ll T$) we find

$$n_\nu + \bar{n}_\nu = \frac{3}{4} n_\gamma + \mathcal{O}\left(\left(\frac{\mu}{T}\right)^2\right) \quad (2.12)$$

and

$$A_\nu = \frac{\pi^2}{12\zeta_3} \frac{\mu}{T} + \mathcal{O}\left(\left(\frac{\mu}{T}\right)^3\right) \approx 0.68 \frac{\mu}{T} + \mathcal{O}\left(\left(\frac{\mu}{T}\right)^3\right), \quad (2.13)$$

where we have used that the chemical potential for antineutrinos is $\bar{\mu} = -\mu$. Of course, these equations are only valid as long as the neutrinos are in thermal equilibrium.

2.3 Helium Abundance

Big Bang nucleosynthesis is a rather complex system depending on a number of parameters, including the baryon asymmetry η and the effective number of neutrino families N_ν^{eff} , or more generally, g_* . This system has been analyzed very thoroughly, including exhaustive numerical calculations. Here we will give a short summary, concentrating on the production of ${}^4\text{He}$.

The outcome of BBN will be abundances of the different species (A, Z) with Z protons and $A - Z$ neutrons. We will express these abundances as the mass fraction contributed by the species, i.e.

$$X_{A,Z} \equiv \frac{A n_{A,Z}}{n_B}, \quad (2.14)$$

where $n_{A,Z}$ and n_B are the number densities of the nuclear species (A, Z) and all baryons, respectively.

In strict thermodynamic equilibrium, the abundances are given by nuclear statistical equilibrium (NSE) so that

$$(X_{A,Z})_{\text{NSE}} \propto \eta^{A-1} \exp\left(\frac{-B_{A,Z}}{T}\right), \quad (2.15)$$

where $B_{A,Z}$ is the binding energy of the nuclear species (A, Z) . We see that the NSE abundances are strongly suppressed by the small baryon asymmetry $\eta \approx 10^{-9}$. This suppression is compensated by the exponential factor in (2.15) at low temperatures $T \ll B_{A,Z}$. For ${}^4\text{He}$, $(X_{\text{He}})_{\text{NSE}} \approx \mathcal{O}(1)$ at $T \approx 0.3$ MeV. Heavier nuclei have significant NSE abundances only at even lower temperatures.

The NSE abundance for an element X will freeze out when the rates $\Gamma(\text{ab} \leftrightarrow \text{X})$ of producing it from the lighter elements a and b become smaller than the expansion rate H . We have

$$\Gamma(\text{ab} \rightarrow \text{X}) \propto n_a n_b \exp \left[-2 \left(\frac{k}{T_{\text{MeV}}} \right)^{1/3} \right], \quad (2.16)$$

where $k \approx Z_a^2 Z_b^2 A_a A_b / (A_a + A_b)$ and $T_{\text{MeV}} = T / \text{MeV}$. The first two factors are the number densities of the nuclear species a and b, respectively, the last factor represents the Coulomb-barrier suppression, which increases with A_i and Z_i . The freeze-out temperatures increase with the Coulomb-barrier suppression.

As the temperature decreases, the NSE abundances increase, but at the same time the nuclear reactions begin to freeze out. Therefore, heavy nuclei are not produced during BBN because they freeze out long before their NSE abundances have become significant.

Apart from traces of other nuclei, BBN produces primarily ${}^4\text{He}$ so that it is a good approximation to assume that all neutrons end up in ${}^4\text{He}$. Then

$$Y \equiv X_{\text{He}} \approx \frac{4n_{\text{He}}}{n_{\text{B}}} = \frac{4(n_{\text{n}}/2)}{n_{\text{n}} + n_{\text{p}}} = \frac{2(n_{\text{n}}/n_{\text{p}})_{\text{BBN}}}{1 + (n_{\text{n}}/n_{\text{p}})_{\text{BBN}}}. \quad (2.17)$$

Therefore, the all-important helium mass fraction Y depends primarily on the n/p ratio at the time when ${}^4\text{He}$ freezes out of NSE, which happens at $t_{\text{BBN}} = 1\text{--}3$ minutes.

To find $(n_{\text{n}}/n_{\text{p}})_{\text{BBN}}$, we have to follow the evolution of the n/p ratio from the beginning. At temperatures above 1 MeV, reactions of the type



maintain chemical equilibrium with the rate $\Gamma \propto G_{\text{F}} T^5$. Therefore

$$\left(\frac{n_{\text{n}}}{n_{\text{p}}} \right) = \exp \left[-\frac{Q}{T} + \frac{\mu_{\text{e}}}{T} - \frac{\mu_{\nu_{\text{e}}}}{T} \right], \quad (2.19)$$

where $Q = 1.293 \text{ MeV}$ is the mass difference between neutrons and protons, and μ_e and μ_{ν_e} are the chemical potentials of the electrons and electron neutrinos, respectively. Surely, μ_e can be neglected since $\mu_e/T \approx \eta \approx 10^{-9}$. For the moment we will set the neutrino asymmetry to zero which is equivalent to $\mu_{\nu_e} = 0$. Then the n/p ratio depends only on the temperature.

At $T_{\text{fr}} \approx 0.8 \text{ MeV}$, the n/p ratio freezes out and thus

$$\left(\frac{n_n}{n_p}\right)_{\text{fr}} \approx \exp(-Q/T_{\text{fr}}) \approx 0.2. \quad (2.20)$$

More exact calculations [8] give $(n_n/n_p)_{\text{fr}} \approx 1/6$.

After freeze-out, the n/p ratio continues to decrease slowly due to neutron decay,

$$n \rightarrow p + e^- + \bar{\nu}_e. \quad (2.21)$$

Therefore,

$$\left(\frac{n_n}{n_p}\right)_{\text{BBN}} \approx \left(\frac{n_n}{n_p}\right)_{\text{fr}} \exp\left[-\ln(2) \frac{t_{\text{BBN}}}{\tau_n}\right] \approx \frac{1}{7}, \quad (2.22)$$

where $\tau_n = 886.7 \pm 1.9 \text{ s}$ is the neutron half-life. If we insert this value into (2.17), we get $Y \approx 0.25$.

2.4 Non-Standard Neutrinos

We now want to derive the influence of neutrinos on the helium abundance. According to (2.19), a non-zero electron neutrino asymmetry changes the n/p ratio by a factor

$$\exp(-\mu_{\nu_e}/T_{\text{fr}}) \approx \exp(-1.5A_{\nu_e}) \approx (1 - 1.5A_{\nu_e}) \quad (2.23)$$

provided that $A_{\nu_e} \ll 1$. As an example, we take $A_{\nu_e} = \pm 0.01$, a realistic value according to [19]. Then (n_n/n_p) is altered by a factor (1 ∓ 0.015) . Of course, this is a very rough estimate, but more detailed works [18, 37] find the same order of magnitude.

A higher effective neutrino number also alters (n_n/n_p) , since it raises g_* , which results in a higher expansion rate H and thus in a higher freeze-out temperature. Taking $N_{\nu}^{\text{eff}} = 4$ instead of 3 as an example, T_{fr} is increased by a factor of

$$\left(\frac{g_*(N_{\nu}^{\text{eff}} = 4)}{g_*(N_{\nu}^{\text{eff}} = 3)}\right)^{1/6} = \left(\frac{10.75 + 2 \cdot \frac{7}{8}}{10.75}\right)^{1/6} = 1.025, \quad (2.24)$$

where the power $1/6$ comes from $\Gamma/H \propto T^3/\sqrt{g_*}$. This changes the n/p ratio by a factor of 1.04.

We insert these changes into (2.17) and expand to get

$$Y \approx 0.25 + 0.01(N_\nu^{\text{eff}} - 3) - 0.33A_{\nu_e} \quad (2.25)$$

if $A_{\nu_e} \ll 1$ and $|N_\nu^{\text{eff}} - 3| \lesssim 1$. We see that $N_\nu^{\text{eff}} = 4$ or $|A_{\nu_e}| = 10^{-2}$ change the helium abundance by several percent, which is within the present experimental precision. More detailed numerical calculations [8] give

$$Y \approx 0.225 + 0.025 \log(\eta/10^{-10}) + 0.012(N_\nu^{\text{eff}} - 3), \quad (2.26)$$

where we have also included the influence of the baryon asymmetry η , since the main uncertainty in Standard BBN comes from this parameter.

We should mention that in the literature, the variable N_ν^{eff} has often been used not only to account for the effective number of neutrinos, but also for the influence of A_{ν_e} . This was done by adding a new term $\delta N_\nu^{\text{eff}}(A_{\nu_e})$ to N_ν^{eff} .

2.5 Observational Results

The best measurements of the primordial ${}^4\text{He}$ abundance, Y , come from observing extra-galactic regions of ionized H. In these systems, the abundance of heavier elements, which are not created in BBN, is very low, so we can assume that the abundances in these regions are close to their primordial values. The present estimate is [6]

$$Y = 0.238 \pm 0.002 \pm 0.005, \quad (2.27)$$

where the two errors are the statistical and systematic errors, respectively. The 2σ range is then estimated [38] to be 0.228–0.248.

Direct present-time measurements of the cosmic baryon abundance are very uncertain due to the dark matter problem. Much better estimates arise from measurements of the primordial Deuterium abundance which depends sensitively on the baryon asymmetry η . The best measurements come from the absorption of quasar light by high-redshift, low-metallicity hydrogen clouds. Two main results have been published [39, 40],

$$(D/H)_{\text{low}} = (3.4 \pm 0.3) \times 10^{-5} \quad \text{and} \quad (D/H)_{\text{high}} = (2 \pm 0.5) \times 10^{-4}, \quad (2.28)$$

which are mutually inconsistent. These two measurements give ranges for the baryon asymmetry of

$$\eta_{\text{low}} = 4.2\text{--}6.3 \times 10^{-10} \quad \text{and} \quad \eta_{\text{high}} = 1.2\text{--}2.8 \times 10^{-10}, \quad (2.29)$$

at a nominal 2σ level.

From the measurements of D/H and Y, one obtains bounds on the effective neutrino number. Olive *et al.* [41] derived

$$(N_{\nu}^{\text{eff}} - 3)_{\text{low}} < 0.3 \quad \text{and} \quad (N_{\nu}^{\text{eff}} - 3)_{\text{high}} < 1.8, \quad (2.30)$$

provided that the ν_e chemical potential can be neglected.

The low-D result today appears to be strongly favored. If it should be confirmed, sterile neutrinos would be forbidden to come into equilibrium for negligible μ_{ν_e} . However, a large positive A_{ν_e} can compensate the effect of an increased N_{ν}^{eff} , and can thus circumvent this constraint.

2.6 Summary

We have shown that a deviation of the effective number of neutrinos of order 1, as well as a ν_e asymmetry exceeding about 10^{-2} , will have a measurable effect on the outcome of BBN. Sterile neutrinos have the potential to change both N_{ν}^{eff} and A_{ν_e} . If we knew how these two variables depend on the mixing parameters of the sterile neutrinos, we could use the measured primordial element abundances to derive constraints on the mixing parameters. On the other hand, if the existence of sterile neutrinos was proven by future experiments such as MiniBooNE [42], a detailed understanding of their impact on primordial nucleosynthesis would be necessary to constrain the free parameters of BBN, in particular the baryon asymmetry η .

Chapter 3

Neutrino Oscillations

Neutrino oscillations play a crucial role in our considerations of the Early Universe involving sterile neutrinos. In this chapter, we derive the density matrix formalism for neutrino oscillations in media between any two neutrino flavors, active or sterile. This includes the direct influence of matter on the vacuum neutrino oscillations as well as scattering processes which tend to destroy the coherence of the oscillations. Our analysis will only be applicable for temperatures between a few MeV and 100 MeV and for neutrino asymmetries $A_\nu \ll 1$.

3.1 Equation of Motion

Neutrino oscillations occur because the basis of the neutrino weak eigenstates ν_α , $\alpha = e, \mu, \tau, s, \dots$, is different from the basis of the neutrino mass eigenstates ν_i , $i = 1, 2, 3, \dots$. In other words, a ν_α that is produced in a weak-interaction process does not propagate like a free particle, but as a superposition of neutrinos ν_i with different masses m_i , respectively. Thus, when measured, the propagated neutrino contains contributions of weak eigenstates other than the original ν_α . From the start we include the possibility that neutrinos exist beyond the active states ν_e , ν_μ and ν_τ . These additional flavors would have to be sterile with regard to the weak interaction.

The two bases are connected by a unitary transformation $\Psi_W = U\Psi_M$,

where

$$\Psi_W \equiv \begin{pmatrix} \Psi_{\nu_e} \\ \Psi_{\nu_\mu} \\ \Psi_{\nu_\tau} \\ \vdots \end{pmatrix} \quad \text{and} \quad \Psi_M \equiv \begin{pmatrix} \Psi_{\nu_1} \\ \Psi_{\nu_2} \\ \Psi_{\nu_3} \\ \vdots \end{pmatrix} \quad (3.1)$$

are the field vectors represented in the weak and mass basis, respectively, and U is the unitary transformation matrix.

We are mainly interested in the evolution of the weak eigenstates, as these are the particles we can produce and measure by weak-interaction processes. Therefore, we write the equation of motion in the basis of the weak eigenstates. The Klein-Gordon equation is

$$(\partial_t^2 - \nabla^2 + M_W^2)\Psi_W = 0, \quad (3.2)$$

where $M_W = UM_M U^\dagger$ and $M_M = \text{diag}(m_1, m_2, \dots)$ is the mass matrix in the weak and mass basis, respectively. Of course, $M_W^2 = UM_M U^\dagger UM_M U^\dagger = UM_M^2 U^\dagger$ and M_W are not diagonal in the case of mixing.

Since the Early Universe is homogeneous, we are only interested in the time evolution of the neutrino fields. It is therefore convenient to expand them in plane waves $\Psi_W = \Psi_p(t)e^{i\mathbf{p}\mathbf{x}}$. Note that usually neutrino oscillations are considered in environments which are spatially inhomogeneous but stationary, e.g. in experiments involving solar or atmospheric neutrinos. In such cases, Ψ_W would be expanded in components of fixed energy, $\Psi_W = \Psi_E(\mathbf{x})e^{-iEt}$, instead of components of fixed momentum.

Since the neutrinos are highly relativistic, $m_\nu \ll E \approx p$, we can linearize the Klein-Gordon equation. Then we get the usual Schrödinger-type equation [43, 44]

$$i\partial_t \Psi_p = \Omega_p \Psi_p, \quad \Omega_p = p + \frac{M_W^2}{2p}. \quad (3.3)$$

We see that the off-diagonal elements of M_W^2 couple the fields of the different neutrino flavors, leading to oscillations.

An equivalent equation is given by

$$i\partial_t \rho = [\rho, \Omega], \quad (3.4)$$

where $\rho_{\alpha\beta} \equiv N\Psi_\alpha \Psi_\beta^\dagger$ is the flavor density matrix, N is a normalization factor, and we have dropped the index p . The advantage of the density matrix

formalism is that we later can include effects that destroy the coherence of the neutrino oscillations.

For later convenience, we normalize the density matrix such that for a CP symmetric neutrino species ν_α in equilibrium, $\rho_{\alpha\alpha} = 1$ for all momentum modes, i.e.

$$n_{\nu_\alpha} = \int \frac{d^3\mathbf{p}}{(2\pi)^3} \Psi_\alpha \Psi_\alpha^\dagger = \int \frac{d^3\mathbf{p}}{(2\pi)^3} f_0(p, T) \rho_{\alpha\alpha}(p), \quad (3.5)$$

where $f_0(p, T) = f(p, T, \mu = 0) = [1 + \exp(p/T)]^{-1}$. Thus, the normalization factor $N = 1/f_0(p, T)$.

We have neglected the expansion of the Universe in the derivation of the equation of motion. It could be included by adding a term $\Omega_H = iHp\partial_p$ to the Hamiltonian. The term disappears if we expand the field vector in comoving plane waves, $\Psi_W = \Psi_q(t)e^{iT\mathbf{q}\mathbf{x}}$, where $q = p/T$, instead of plane waves with fixed momentum. Therefore, later in Chapter 4 we will not describe the evolution of flavor density matrices of fixed momentum p , but of fixed comoving momentum q .

3.2 Medium Effects

In the Early Universe, we are confronted with a thermal medium which interacts with the neutrinos. Therefore, we need to include the effects of these interactions on the neutrino oscillations. In this section, we restrict ourselves to the discussion of the refractive effects [45].

The medium contributions to the neutrino oscillations enter the Schrödinger equation (3.3) through the weak-potential term $V \equiv \text{diag}(V_{\nu_\alpha}, V_{\nu_\beta}, \dots)$ in

$$\Omega = p + \frac{M_W^2}{2p} + V. \quad (3.6)$$

For each neutrino weak eigenstate the contributions can be split into two terms,

$$V_{\nu_\alpha} = \pm V_{\nu_\alpha}^A - V_{\nu_\alpha}^T. \quad (3.7)$$

Here, the plus sign is valid for neutrinos, while the minus sign applies to antineutrinos.

The first term accounts for the fermion asymmetries. For neutrinos of species α it is given by [45]

$$V_{\nu_\alpha}^A = \sqrt{2}G_F n_\gamma \tilde{A}_{\nu_\alpha}, \quad (3.8)$$

where $G_F = 1.166 \times 10^{-5} \text{ GeV}^{-2}$ is Fermi's constant and \tilde{A}_{ν_α} a weighted sum over all fermion asymmetries A_i . Generally,

$$\begin{aligned}\tilde{A}_{\nu_\alpha} &= A_{\nu_\alpha} + A_{\nu_e} + A_{\nu_\mu} + A_{\nu_\tau} \\ &\quad + A_\alpha - \frac{1}{2}(1 - 4 \sin^2 \theta_W)(A_e + A_\mu + A_\tau) \\ &\quad + \frac{1}{2}(1 - 4 \sin^2 \theta_W)A_p - \frac{1}{2}A_n,\end{aligned}\tag{3.9}$$

where θ_W is the Weinberg angle. For our assumption of a charge-neutral Universe we have $A_e + A_\mu + A_\tau = A_p$ and therefore

$$\tilde{A}_{\nu_\alpha} = A_{\nu_\alpha} + A_{\nu_e} + A_{\nu_\mu} + A_{\nu_\tau} - \frac{1}{2}A_n + A_\alpha.\tag{3.10}$$

Since the muons and tauons are non-relativistic, their asymmetries are negligible, so that we will use $A_e = A_p$, $A_\mu = 0$, and $A_\tau = 0$. In our analysis, all of the asymmetries but for one type of neutrino will remain constant. Therefore, we write

$$\tilde{A}_{\nu_\alpha} = 2A_{\nu_\alpha} + A_c,\tag{3.11}$$

where all asymmetries other than A_{ν_α} have been absorbed in a constant A_c .

The second term in (3.7) represents the low-energy tail of the W^\pm and Z^0 resonances. It has the remarkable feature that it is independent of the CP asymmetry of the background medium and has the same effect on neutrinos and antineutrinos. Since it is of order G_F^2 , V^T can only compete with V^A in the Early Universe, where $A \ll 1$. For neutrino temperatures far below the W^\pm and Z^0 -masses it can be written in the form [45]

$$V_{\nu_\alpha}^T = z_{\nu_\alpha} G_F^2 p T n_\gamma.\tag{3.12}$$

Here, the coefficients are

$$\begin{aligned}z_{\nu_e} &= \frac{7\pi^3}{45\zeta_3\alpha} \sin^2 \theta_W (\cos^2 \theta_W + 2) \approx 350 \\ z_{\nu_\mu, \nu_\tau} &= \frac{7\pi^3}{45\zeta_3\alpha} \sin^2 \theta_W \cos^2 \theta_W \approx 97,\end{aligned}\tag{3.13}$$

where $\alpha = 1/137$ is the fine-structure constant.

Since we will be discussing sterile neutrinos, we stress their special role in a medium. They do not interact, so $V_{\nu_s} = 0$. Likewise, a possible asymmetry A_{ν_s} does not contribute to $V_{\nu_\alpha}^A$ for the active flavor.

3.3 Density Matrix Formalism for Two-Flavor Oscillations

We will now treat the simplest case of neutrino oscillations between two types of neutrinos, so $\Psi_W = (\Psi_{\nu_\alpha}, \Psi_{\nu_\beta})$. The unitary transformation can be written in the simple form

$$U = \begin{pmatrix} \cos \theta & -\sin \theta \\ \sin \theta & \cos \theta \end{pmatrix}, \quad (3.14)$$

where θ is the vacuum mixing angle. Note that the absolute phase of the off-diagonal terms is arbitrary; our convention differs from some of the literature. In the weak basis we get

$$\Omega = \frac{1}{2} b I - \frac{1}{2} \begin{pmatrix} c\Delta + \delta V & s\Delta \\ s\Delta & -(c\Delta + \delta V) \end{pmatrix}, \quad (3.15)$$

where $b = 2p + \frac{m_1^2 + m_2^2}{2p} - (V_{\nu_\alpha} + V_{\nu_\beta})$, I is the 2×2 unit matrix, and $\delta V = V_{\nu_\alpha} - V_{\nu_\beta}$. Furthermore, we have defined

$$s \equiv \sin 2\theta, \quad c \equiv \cos 2\theta, \quad \Delta \equiv \frac{\delta m^2}{2p} \quad (3.16)$$

with the mass squared difference $\delta m^2 \equiv m_2^2 - m_1^2$.

To find a convenient form for the equation of motion, we represent ρ and Ω by the unit matrix I and the Pauli matrices σ_i , $i = 1, 2, 3$ [44]. Then

$$\rho = \frac{1}{2} P_0 I + \frac{1}{2} \mathbf{P} \boldsymbol{\sigma}, \quad \Omega = \frac{1}{2} b I - \frac{1}{2} \mathbf{B} \boldsymbol{\sigma}, \quad (3.17)$$

where \mathbf{P} is a so-called flavor polarization vector, and

$$\mathbf{B} = \begin{pmatrix} s\Delta & \\ & 0 \\ c\Delta + \delta V & \end{pmatrix}. \quad (3.18)$$

Inserting ρ and Ω into (3.4) and using the commutation relation for the Pauli matrices, $[\frac{1}{2}\sigma_i, \frac{1}{2}\sigma_j] = i\epsilon_{ijk}\frac{1}{2}\sigma_k$, we derive

$$\partial_t \mathbf{P} = \mathbf{B} \times \mathbf{P}. \quad (3.19)$$

This equation is equivalent to the precession of a spin vector in a magnetic field. The physical observables are now contained in $P_z = \rho_{\alpha\alpha} - \rho_{\beta\beta}$ and

$P_0 = \rho_{\alpha\alpha} + \rho_{\beta\beta}$. $f_0(p, T)P_0$ is the total occupation number of both ν_α and ν_β of momentum mode p , while P_z represents the difference between the two neutrino types; if e.g. $P_z = 1$ for all modes, then $n_{\nu_\beta} = 0$. However, if $P_z = 0$ for all modes, $n_{\nu_\alpha} = n_{\nu_\beta}$. The other two components $P_{x,y}$ represent the phase of the oscillations.

3.4 Scattering Processes

We must still take into account that the weak neutrino eigenstates scatter on the background plasma with the rate [46]

$$\Gamma_{\nu_\alpha} = y_{\nu_\alpha} G_F^2 p T^4, \quad (3.20)$$

where $y_{\nu_e} \approx 1.13$, $y_{\nu_\mu, \nu_\tau} \approx 0.79$ and $y_{\nu_s} \equiv 0$. To be precise, y_{ν_α} also depends on the momentum due to the Pauli blocking factors. We will use these momentum averaged values [24].

Scattering keeps the active neutrinos in thermal and chemical equilibrium at temperatures above a few MeV. Therefore, the integrand in (3.5), $f_0(p, T)\rho_{\alpha\alpha}(p)$, should be equal to $f(p, T, \mu)$. However, $\rho_{\alpha\alpha}(p)$ changes due to the neutrino oscillations. The scattering processes compensate this change by re- or depopulating the number densities through $\dot{\rho}_{\alpha\alpha}(p) = R_{\nu_\alpha}(p)$, where the rate is approximately given by [46]

$$R_{\nu_\alpha}(p) \approx \Gamma_{\nu_\alpha} \left[\frac{f(p, T, \mu)}{f_0(p, T)} - \rho_{\alpha\alpha}(p) \right]. \quad (3.21)$$

The approximation holds as long as the deviation from equilibrium is small. Of course, $R_{\nu_s} = \Gamma_{\nu_s} = 0$.

A much more interesting effect appears if the scattering rates are different for the two neutrino types considered. Then scattering distinguishes between the two ν types and thus the coherence of the neutrino oscillations is destroyed. Therefore, we need to include a term $-D\mathbf{P}_\perp(p)$, where $\mathbf{P}_\perp = (P_x, P_y, 0)$ and D is called the damping rate. In the case of an active neutrino oscillating with a sterile neutrino ($\beta = s$) we have $D = \frac{1}{2}\Gamma_{\nu_\alpha}$. The lengthy derivation of this term can be read in [47].

In summary, for each neutrino momentum mode p we have derived a system of differential equations

$$\partial_t \mathbf{P} = \mathbf{B} \times \mathbf{P} - D\mathbf{P}_\perp + (R_{\nu_\alpha} - R_{\nu_\beta})\hat{\mathbf{z}}, \quad (3.22)$$

$$\partial_t P_0 = (R_{\nu_\alpha} + R_{\nu_\beta}), \quad (3.23)$$

$$\partial_t \bar{\mathbf{P}} = \bar{\mathbf{B}} \times \bar{\mathbf{P}} - D\bar{\mathbf{P}}_{\perp} + (\bar{R}_{\nu_{\alpha}} - \bar{R}_{\nu_{\beta}})\hat{\mathbf{z}}, \quad (3.24)$$

$$\partial_t \bar{P}_0 = (\bar{R}_{\nu_{\alpha}} + \bar{R}_{\nu_{\beta}}), \quad (3.25)$$

where $\hat{\mathbf{z}} = (0, 0, 1)$. In the next chapter we will study the highly non-trivial behavior of this equation of motion.

Chapter 4

Oscillating Lepton Asymmetry

We analyze the system of flavor oscillations between active and sterile neutrinos before BBN in a simplified model. First we discuss our approximations and present a typical numerical solution of the simplified model. Next, we introduce a more convenient coordinate system for the analytical treatment. With its help, we describe the evolution of our system from very early times up to the resonance. At resonance, we show that we can describe the evolution of the neutrino asymmetry with a simple differential equation, and that the solution will indeed oscillate for some of the parameter space.

4.1 Simplified Model

We describe the oscillations between two flavors of neutrinos, one active and one sterile, in an expanding medium. This means that we neglect all other neutrino mixings, which is a good approximation if all other effective mixing angles are small. Thus, we can describe our oscillations by the system of differential equations (3.22)–(3.25) derived in the previous chapter. We restrict ourselves to a simplified model which we present in this section. For definiteness, we will analyze the case where the active neutrino is ν_τ ; the analysis is analogous for ν_e and ν_μ .

Our most important simplification is that we neglect the momentum distribution. This is surely not a good approximation, since then all neutrinos encounter the oscillation resonance at the same time. In reality only a small fraction of the neutrinos will be simultaneously at resonance, especially when the resonance width is small, i.e. the vacuum mixing angle is small. However,

the complete system is very complicated, as can be seen from the controversial literature on its solution, and we therefore have decided to analyze this simplified model. Of course, it is desirable to include the effects of the momentum distribution in future investigations.

So from now on, all neutrinos are taken to have the same momentum. We choose this momentum to be the average of a fermion species with vanishing chemical potential,

$$\langle p \rangle = \frac{7\zeta_4}{2\zeta_3} T \approx 3.15 T, \quad (4.1)$$

where ζ is the Riemann zeta function with $\zeta_3 \approx 1.202$ and $\zeta_4 = \pi^4/90$. As a consequence, we only have two density matrices, $\rho_{\alpha\alpha}$ for the neutrinos and $\bar{\rho}_{\alpha\alpha}$ for the antineutrinos. We normalize these in analogy to our previous normalization in Section 3.1, i.e. such that the number densities are $n_{\nu_\tau} = n_\nu^{\text{eq}} \rho_{\tau\tau}$, etc. where $n_\nu^{\text{eq}} = \frac{3}{8} n_\gamma$ is the equilibrium neutrino number density for vanishing chemical potential.

We will also neglect the repopulation terms R_{ν_τ} and \bar{R}_{ν_τ} defined in (3.21). They will be small if the ν_τ and $\bar{\nu}_\tau$ are not depopulated significantly by neutrino oscillations, and if $A_{\nu_\tau} \ll 1$ so that the chemical potential has no significant influence on the equilibrium number density. This simplification is valid for some part of the parameter space, which we will determine later. As a result of this approximation, P_0 and \bar{P}_0 are constant in time.

So now, the system of differential equations has been simplified to

$$\begin{aligned} \partial_t \mathbf{P} &= \mathbf{B} \times \mathbf{P} - DP_\perp, \\ \partial_t \bar{\mathbf{P}} &= \bar{\mathbf{B}} \times \bar{\mathbf{P}} - D\bar{P}_\perp. \end{aligned} \quad (4.2)$$

The tau neutrino asymmetry

$$A_{\nu_\tau} = \frac{n_{\nu_\tau}^{\text{eq}}}{n_\gamma} (\rho_{\tau\tau} - \bar{\rho}_{\tau\tau}) = \frac{3}{8} \times \frac{1}{2} (P_z - \bar{P}_z + P_0 - \bar{P}_0) \quad (4.3)$$

is an important variable since it depends on \mathbf{P} , enters into \mathbf{B} , and thus causes the system to be nonlinear. It will be more convenient to use the equivalent variable

$$\delta P_z \equiv \frac{4}{3} \tilde{A}_{\nu_\tau} = \frac{1}{2} (P_z - \bar{P}_z) + P_c, \quad (4.4)$$

where \tilde{A}_{ν_τ} was given in (3.10) and $P_c \equiv \frac{4}{3} (A_{\nu_e} + A_{\nu_\mu} - \frac{1}{2} A_n) + \frac{1}{2} (P_0 - \bar{P}_0)$ is constant.

In terms of this variable, the coefficients in the differential equations are given by

$$\mathbf{B}(T, \delta P_z) = \begin{pmatrix} -b_s \\ 0 \\ -b_c + b_T - b_A \delta P_z \end{pmatrix}, \quad (4.5)$$

$$\bar{\mathbf{B}}(T, \delta P_z) = \begin{pmatrix} -b_s \\ 0 \\ -b_c + b_T + b_A \delta P_z \end{pmatrix}, \quad (4.6)$$

where we use

$$\begin{aligned} b_s &\equiv -\frac{s \delta m^2}{2 \langle p \rangle} \approx -\frac{s \delta m^2}{6.3} T^{-1}, \\ b_c &\equiv -\frac{c \delta m^2}{2 \langle p \rangle} \approx -\frac{c \delta m^2}{6.3} T^{-1}, \\ b_A &\equiv V_{\nu_\tau}^A / \delta P_z = k_A T^3, \\ b_T &\equiv V_{\nu_\tau}^T = k_T T^5. \end{aligned} \quad (4.7)$$

Recall that $s = \sin 2\theta$, $c = \cos 2\theta$, and $\delta m^2 = m_{\nu_s}^2 - m_{\nu_\tau}^2$. The constants are

$$\begin{aligned} k_A &= \frac{3\zeta_3}{4\pi^2} \sqrt{2} G_F \approx 1.51 \times 10^{-24} \text{ eV}^{-2}, \\ k_T &= \frac{14\pi}{45\alpha} \sin^2 \theta_W \cos^2 \theta_W \frac{\langle p \rangle}{T} G_F^2 \approx 1.02 \times 10^{-44} \text{ eV}^{-4}, \end{aligned} \quad (4.8)$$

where $\alpha = 1/137$ is the fine-structure constant and θ_W the Weinberg angle. The coefficient D is proportional to b_T , so we will often use the relation

$$D = k_D b_T, \quad (4.9)$$

where

$$k_D = \frac{\pi^2 y_{\nu_\tau}}{2\zeta_3 z_{\nu_\tau}} \approx 1/60, \quad (4.10)$$

and we have used $y_{\nu_\tau} \approx 0.79$ and $z_{\nu_\tau} \approx 97$ from Section 3.2. For ν_μ , the constants are the same. For ν_e , we have $k_T \approx 3.66 \times 10^{-44} \text{ eV}^{-4}$ and $k_D \approx 1/151$.

We will be considering neutrino oscillations with small vacuum mixing angles, i.e. $s \ll c \approx 1$. As a consequence, the first component of \mathbf{B} will be

much smaller than the third component for most of the time. The system becomes interesting when the third component disappears. Then the neutrino oscillations are at resonance, i.e. the neutrinos mix maximally. If we assume the initial asymmetry to be negligible, the resonance condition is given by $b_c = b_T$. This condition has a solution only if $\delta m^2 < 0$. Then resonance occurs when

$$T_{\text{res}} = \left(\frac{|\delta m^2| c}{6.3 k_T} \right)^{1/6} \approx 15.8 \text{ MeV} |\delta m_{\text{eV}}^2|^{1/6}, \quad (4.11)$$

where $\delta m_{\text{eV}}^2 = \delta m^2 / \text{eV}^2$. The resonance will be the crucial feature of the system. We will see that shortly after the resonance, the neutrino oscillations will create a large asymmetry, an effect which is driven by the non-linear term $b_A \delta P_z$ in the system of differential equations. We will therefore only consider $\delta m^2 < 0$, i.e. the sterile neutrino is lighter than the tau neutrino.

4.2 Numerical Solution

We have solved the system (4.2) of differential equations numerically and find results similar to those in [21] and [22]. We have plotted the evolution of the effective asymmetry δP_z for $(\delta m^2, s) = (-1 \text{ eV}^2, 10^{-4})$ in Fig. 4.1. Its behavior is representative for a large region of parameter space. The evolution of the system falls into five distinct phases.

1. At high temperatures, the asymmetry δP_z is constant, since damping totally destroys the coherence of the oscillations. Thus, no flavor transition occurs at all.
2. As the temperature decreases, the mixing angle increases, while the damping rate decreases. As a consequence, there will be a small amount of flavor transition induced by the damping. Due to the asymmetric term $b_A \delta P_z$, this transition rate will be different for neutrinos and antineutrinos, washing out the asymmetry δP_z . However, there remains a small relic asymmetry.
3. Until the system reaches the resonance, the relic asymmetry changes slowly.
4. When the system has passed the resonance, the difference in the transition rates for neutrinos and antineutrinos has the opposite effect than

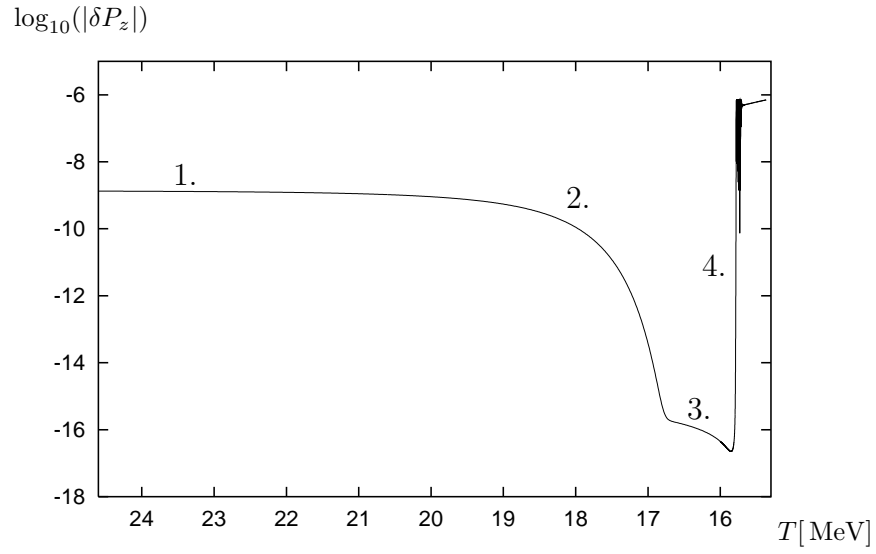


Figure 4.1: Evolution of δP_z , steps 1. to 4.

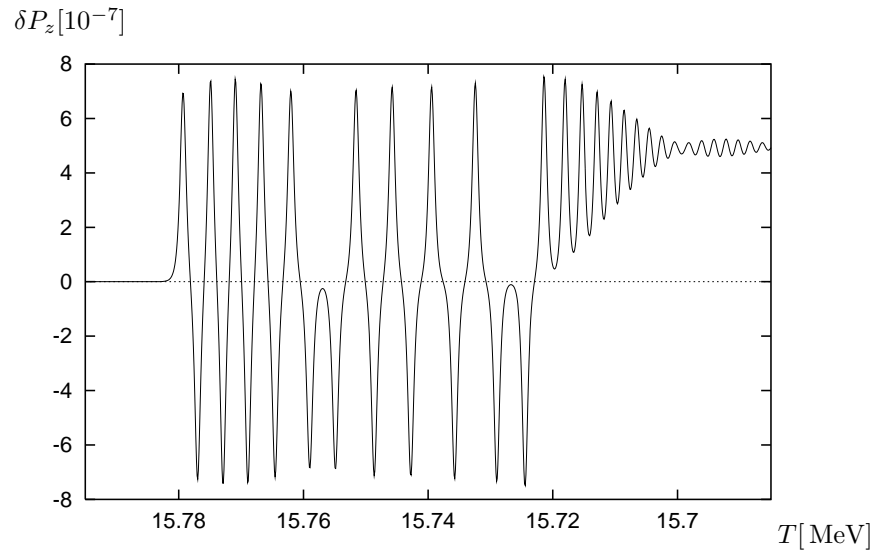


Figure 4.2: Oscillatory behavior of δP_z during step 5.

before. In other words, a small asymmetry is no longer washed out, but amplified, which leads to an exponential increase of δP_z .

5. When $\delta P_z = \mathcal{O}(10^{-6})$, it starts oscillating and thereby even changes its sign. For our numerical example, we have plotted the evolution of δP_z during this step in Fig. 4.2.
6. Eventually, the neutrino asymmetry stops oscillating. After that, it slowly increases.

In the past, the underlying mechanism for the oscillatory behavior in step 5 was not fully understood. Merely the authors of [21] discussed this phenomenon qualitatively. Our main achievement will be to analyze the system analytically and to prove that it indeed oscillates. Thus, we invalidate the frequently used argument that the oscillations in this phase are an artifact caused by a numerical instability.

4.3 Spherical Coordinates

We will now change to a more convenient coordinate system. The two phase-related coordinates P_x and P_y are not very practical, so we prefer to use spherical coordinates. As a measure for the length $P = |\mathbf{P}|$ of the polarization vector we use P_z because it enters directly into (4.4). This choice becomes problematic when $P_z = 0$, $P \neq 0$, but as mentioned above, P_z will not change significantly. The new coordinate system consists of P_z and the angles ϑ and φ . These new variables are related to the old ones as

$$\begin{aligned} P_x &= P_z \tan \vartheta \sin \varphi, \\ P_y &= P_z \tan \vartheta \cos \varphi, \\ P_z &= P_z. \end{aligned} \tag{4.12}$$

P_z represents the relation between the number densities of the active and sterile neutrinos, ϑ is a measure of how much the polarization vector deviates from the z -axis, and φ is the rotation angle around the z -axis. Then the differential equations (4.2) change to

$$\begin{aligned} \dot{P}_z &= -b_s P_z \tan \vartheta \cos \varphi, \\ \dot{\vartheta} &= -D \sin \vartheta \cos \vartheta + b_s \cos \varphi, \\ \dot{\varphi} &= b_c - b_T + b_A \delta P_z - b_s \cot \vartheta \sin \varphi, \end{aligned} \tag{4.13}$$

and

$$\begin{aligned}
\dot{\bar{P}}_z &= -b_s \bar{P}_z \tan \bar{\vartheta} \cos \bar{\varphi}, \\
\dot{\bar{\vartheta}} &= -D \sin \bar{\vartheta} \cos \bar{\vartheta} + b_s \cos \bar{\varphi}, \\
\dot{\bar{\varphi}} &= b_c - b_T - b_A \delta P_z - b_s \cot \bar{\vartheta} \sin \bar{\varphi},
\end{aligned} \tag{4.14}$$

where over-barred quantities, as usual, refer to antineutrinos. With (4.4) we have a closed set of differential equations.

The only difference between the equations for neutrinos and antineutrinos is the sign of the term $b_A \delta P_z$. Therefore, if this term is negligible, the variables for neutrinos and antineutrinos develop equally. To be more sensitive to the small differences induced by the asymmetry, we perform another substitution and use the variables

$$\begin{aligned}
P_z^\pm &\equiv \frac{1}{2}(P_z \pm \bar{P}_z), \\
\vartheta^\pm &\equiv \frac{1}{2}(\vartheta \pm \bar{\vartheta}), \\
\varphi^\pm &\equiv \frac{1}{2}(\varphi \pm \bar{\varphi})
\end{aligned} \tag{4.15}$$

instead. Thus $P_z^+ \gg P_z^-$, $\vartheta^+ \gg \vartheta^-$ and $\varphi^+ \gg \varphi^-$ when the fermion asymmetry is small. Note that (4.4) becomes

$$\delta P_z(t) = P_z^-(t) + P_c \tag{4.16}$$

so that $\frac{d}{dt} \delta P_z = \dot{P}_z^-$. We will make use of this simple relation by considering δP_z instead of P_z^- when it is convenient.

In terms of the new variables, our system of differential equations is

$$\begin{aligned}
\dot{P}_z^+ &= -b_s P_z^+ \frac{\sin 2\vartheta^+ \cos \varphi^+ \cos \varphi^- - \sin 2\vartheta^- \sin \varphi^+ \sin \varphi^-}{\cos 2\vartheta^+ + \cos 2\vartheta^-} \\
&\quad - b_s P_z^- \frac{-\sin 2\vartheta^+ \sin \varphi^+ \sin \varphi^- + \sin 2\vartheta^- \cos \varphi^+ \cos \varphi^-}{\cos 2\vartheta^+ + \cos 2\vartheta^-}, \tag{4.17}
\end{aligned}$$

$$\begin{aligned}
\dot{P}_z^- &= -b_s P_z^+ \frac{-\sin 2\vartheta^+ \sin \varphi^+ \sin \varphi^- + \sin 2\vartheta^- \cos \varphi^+ \cos \varphi^-}{\cos 2\vartheta^+ + \cos 2\vartheta^-} \\
&\quad - b_s P_z^- \frac{\sin 2\vartheta^+ \cos \varphi^+ \cos \varphi^- - \sin 2\vartheta^- \sin \varphi^+ \sin \varphi^-}{\cos 2\vartheta^+ + \cos 2\vartheta^-}, \tag{4.18}
\end{aligned}$$

$$\dot{\vartheta}^+ = -\frac{1}{2} D \sin 2\vartheta^+ \cos 2\vartheta^- + b_s \cos \varphi^+ \cos \varphi^-, \tag{4.19}$$

$$\dot{\vartheta}^- = -\frac{1}{2} D \cos 2\vartheta^+ \sin 2\vartheta^- - b_s \sin \varphi^+ \sin \varphi^-, \tag{4.20}$$

$$\begin{aligned}\dot{\varphi}^+ &= b_c - b_T \\ &+ b_s \frac{-\sin 2\vartheta^+ \sin \varphi^+ \cos \varphi^- + \sin 2\vartheta^- \cos \varphi^+ \sin \varphi^-}{\cos 2\vartheta^- - \cos 2\vartheta^+},\end{aligned}\quad (4.21)$$

$$\begin{aligned}\dot{\varphi}^- &= b_A(P_z^- + P_c) \\ &+ b_s \frac{-\sin 2\vartheta^+ \cos \varphi^+ \sin \varphi^- + \sin 2\vartheta^- \sin \varphi^+ \cos \varphi^-}{\cos 2\vartheta^- - \cos 2\vartheta^+}.\end{aligned}\quad (4.22)$$

As a last approximation, we assume $\vartheta^\pm \ll 1$, which effectively means that the polarization vectors will stay close to the z -axis. We expand $\sin 2\vartheta^\pm$ and $\cos 2\vartheta^\pm$ and only take into account the leading order terms. Then we get

$$\begin{aligned}\dot{P}_z^+ &= -b_s P_z^+ \left(\vartheta^+ \cos \varphi^+ \cos \varphi^- - \vartheta^- \sin \varphi^+ \sin \varphi^- \right) \\ &- b_s P_z^- \left(-\vartheta^+ \sin \varphi^+ \sin \varphi^- + \vartheta^- \cos \varphi^+ \cos \varphi^- \right),\end{aligned}\quad (4.23)$$

$$\begin{aligned}\dot{P}_z^- &= -b_s P_z^+ \left(-\vartheta^+ \sin \varphi^+ \sin \varphi^- + \vartheta^- \cos \varphi^+ \cos \varphi^- \right) \\ &- b_s P_z^- \left(\vartheta^+ \cos \varphi^+ \cos \varphi^- - \vartheta^- \sin \varphi^+ \sin \varphi^- \right),\end{aligned}\quad (4.24)$$

$$\dot{\vartheta}^+ = -D\vartheta^+ + b_s \cos \varphi^+ \cos \varphi^-, \quad (4.25)$$

$$\dot{\vartheta}^- = -D\vartheta^- - b_s \sin \varphi^+ \sin \varphi^-, \quad (4.26)$$

$$\begin{aligned}\dot{\varphi}^+ &= b_c - b_T \\ &+ \frac{b_s}{\vartheta^+} \left(-\sin \varphi^+ \cos \varphi^- + \frac{\vartheta^-}{\vartheta^+} \cos \varphi^+ \sin \varphi^- \right),\end{aligned}\quad (4.27)$$

$$\begin{aligned}\dot{\varphi}^- &= b_A(P_z^- + P_c) \\ &+ \frac{b_s}{\vartheta^+} \left(-\cos \varphi^+ \sin \varphi^- + \frac{\vartheta^-}{\vartheta^+} \sin \varphi^+ \cos \varphi^- \right).\end{aligned}\quad (4.28)$$

From (4.25) we see that $\dot{\vartheta}^+ \leq -D\vartheta^+ + b_s$. Thus $\vartheta^+ \geq b_s/D$ would automatically mean that $\dot{\vartheta}^+ \leq 0$. Therefore, we can safely say that $\vartheta^+ < b_s/D$ at all times. We will see that ϑ^+ becomes maximal at resonance, so $\vartheta_{\max}^+ \approx (b_s/D)_{\text{res}} = s/(ck_D)$, where we have used $b_s/s = b_c/c$, $(b_c)_{\text{res}} = (b_T)_{\text{res}}$ and $D = k_D b_T$. Thus our approximation is only valid if $s \ll k_D = 1/60$, $c \approx 1$, i.e. for small mixing angles.

4.4 Initial Conditions

We need to derive the initial conditions before we can consider the evolution of the system of differential equations. We begin with temperatures far above the resonance. For $T \rightarrow \infty$, the coefficients D , b_T , $R_{\nu_\tau} \propto T^5 \rightarrow \infty$, $b_A \propto T^3 \rightarrow \infty$, while b_s , $b_c \propto T^{-1} \rightarrow 0$. If we compare these coefficients with $H \propto T^2$, we conclude that b_s and b_c can be neglected at very high temperatures. Thus, from (4.23)–(4.26) we see that regardless of the initial conditions, ϑ^+ and ϑ^- are both exponentially damped to zero, while $P_z^\pm \propto b_s$ do not change. However, the scattering processes equilibrate ν_τ and $\bar{\nu}_\tau$, implying $\rho_{\tau\tau}$ and $\bar{\rho}_{\tau\tau} \rightarrow 1$. Since the sterile neutrinos do not interact, ρ_{ss} and $\bar{\rho}_{ss}$ remain constant. They are only diluted whenever massive particles become non-relativistic and annihilate into the still relativistic particles, which heats up the plasma. For example, when the temperature decreases from $T \sim \text{TeV}$ (just before the electro-weak symmetry breaking) to $T \sim \text{MeV}$ (shortly after the quark-hadron phase transition), ρ_{ss} and $\bar{\rho}_{ss}$ are diluted by a factor of $[g_*(T \sim 300 \text{ MeV})/g_*(T \sim \text{TeV})]^{4/3} \sim 0.07$. So if the ν_s were in equilibrium with the thermal plasma at very early times by some unknown mechanism, they would have been strongly diluted by the time they become interesting for us. We will simply assume that their initial density is zero. Then the initial conditions are $P_0 = \bar{P}_0 = 1$ and $P_z = \bar{P}_z = 1$. Including the small initial neutrino asymmetries, A_{ν_τ} and A_{ν_s} , we find

$$\begin{aligned}
 P_z^+ &= 1, \\
 P_z^- &= \frac{4}{3}(A_{\nu_\tau} - A_{\nu_s}), \\
 \frac{1}{2}(P_0 - \bar{P}_0) &= \frac{4}{3}(A_{\nu_\tau} + A_{\nu_s}) = \text{const}, \\
 P_c &= \frac{4}{3}(A_c + A_{\nu_\tau} + A_{\nu_s}) = \text{const}, \tag{4.29}
 \end{aligned}$$

where in P_z^+ we have neglected A_{ν_τ} and $A_{\nu_s} \ll 1$.

4.5 Quasi-Static Solutions

We will now follow the time evolution of the system. We first stress the important role that damping plays in our system. We consider a variable x ,

which follows the differential equation

$$\frac{\partial}{\partial t}x(t) = -d(t)x(t) + f(t), \quad (4.30)$$

where $d(t)$ is some damping coefficient and $f(t)$ is a function. If d and f are constant, x will relax to a static value $x_{\text{st}} = \frac{f}{d}$. In our case, d and f will slowly vary in time, and so will the static value. But if its rate of change $r_x \equiv \dot{x}_{\text{st}}/x_{\text{st}}$ is smaller than the damping coefficient d , the damping will force the variable to follow its static value. We will make use of this approximation; since it is not static in the strict sense of the meaning, we will call these solutions quasi-static.

We have calculated the rates of change of the quasi-static solutions for our variables in Appendix A. For the discussion in this section it is sufficient to know that $r = \mathcal{O}(H)$.

We can now determine the variables for large temperatures. We can easily assume that $b_s\vartheta^\pm \ll D\vartheta^\pm, b_s, (b_c - b_T), b_s/\vartheta^\pm$, so before P_z^\pm change significantly at all, the other four variables will have relaxed to their quasi-static values. If we assume that $\dot{P}_z^- = 0$, the differential equations for neutrinos and antineutrinos (4.2) decouple. For small ϑ , the angular equations in (4.13) become

$$\dot{\vartheta} = -D\vartheta + b_s \cos \varphi \quad (4.31)$$

$$\dot{\varphi} = (b_c - b_T + b_A\delta P_z) - \frac{b_s}{\vartheta} \sin \varphi. \quad (4.32)$$

Since $\vartheta > 0$ by definition, the first term in the first equation and the second term in the second equation are both damping terms. The two variables relax to $\dot{\vartheta} \approx \dot{\varphi} \approx 0$ if the quasi-static conditions are fulfilled, i.e. $D > H$ and $b_s/\vartheta > H$, respectively. The first condition is fulfilled for $T > \text{few MeV}$. When ϑ has relaxed, we get from (4.31) that $\vartheta \approx b_s \cos \varphi / D < b_s / D$, which fulfills the second condition, $b_s/\vartheta > D > H$. Setting $\dot{\vartheta} = \dot{\varphi} = 0$, we get the quasi-static solutions

$$\vartheta_{\text{qs}} = \frac{b_s}{\sqrt{D^2 + (b_c - b_T + b_A\delta P_z)^2}}, \quad (4.33)$$

$$\varphi_{\text{qs}} = \arctan\left(\frac{b_c - b_T + b_A\delta P_z}{D}\right). \quad (4.34)$$

The same is valid for the antineutrinos, but with $\delta P_z \rightarrow -\delta P_z$. Since $b_A \delta P_z \ll b_c - b_T$, we can already say that the variables ϑ^- and φ^- will be much smaller than ϑ^+ and φ^+ , respectively. Thus,

$$\vartheta_{\text{qs}}^+ = \frac{1}{2}(\vartheta_{\text{qs}} + \bar{\vartheta}_{\text{qs}}) \approx \frac{b_s}{\sqrt{D^2 + (b_c - b_T)^2}}, \quad (4.35)$$

$$\varphi_{\text{qs}}^+ = \frac{1}{2}(\varphi_{\text{qs}} + \bar{\varphi}_{\text{qs}}) \approx \arctan\left(\frac{b_c - b_T}{D}\right). \quad (4.36)$$

The same quasi-static solutions are also derived from (4.25) and (4.27) if we neglect the last term in latter.

Now it is also easy to calculate ϑ^- and φ^- for a given δP_z by setting $\dot{\vartheta}^- = 0$ in (4.26) and $\dot{\varphi}^- = 0$ in (4.28), inserting ϑ_{qs}^+ and φ_{qs}^+ and setting $\cos \varphi^- = 1$. Then

$$\varphi_{\text{qs}}^- = \arcsin\left(\frac{Db_A}{D^2 + (b_c - b_T)^2} \delta P_z\right) \quad (4.37)$$

$$\vartheta_{\text{qs}}^- = \frac{-b_s(b_c - b_T)b_A}{[D^2 + (b_c - b_T)^2]^{3/2}} \delta P_z. \quad (4.38)$$

Again, we need to show that the quasi-static conditions are fulfilled, which we again find to be $D > H$.

If we insert all these variables into \dot{P}_z^- , and neglect the fourth term in (4.24), we obtain

$$\frac{d}{dt} \delta P_z = \dot{P}_z^- = -\kappa(\delta P_z + \varepsilon P_z^-), \quad (4.39)$$

where the damping coefficient is

$$\kappa \equiv \left| \frac{2P_z^+ b_s^2 (b_c - b_T) D b_A}{[D^2 + (b_c - b_T)^2]^2} \right| \propto T^{-9}, \quad (4.40)$$

and

$$\varepsilon \equiv \left| \frac{D^2 + (b_c - b_T)^2}{2P_z^+ b_A (b_c - b_T)} \right|, \quad (4.41)$$

where $\varepsilon \ll 1$ for $T < \text{GeV}$ and $T \neq T_{\text{res}}$. Analogously, we get

$$\dot{P}_z^+ = -\kappa \varepsilon P_z^+ \propto T^{-7}, \quad (4.42)$$

where we have only taken into account the first term in (4.23), since the other terms are all $\mathcal{O}(P_z^-)$ smaller. This confirms that P_z^- and P_z^+ will not relax to their quasi-static values at high temperatures.

4.6 Evolution Towards the Resonance

When $\kappa \gtrsim H$, δP_z starts changing. The damping coefficients for φ^- and ϑ^- (which are $\gtrsim D$) are much larger than H , so even though δP_z changes, (4.37) and (4.38) remain valid.

From (4.39) we see that δP_z is damped towards 0, i.e. $P_z^- \rightarrow -P_c$. When $|\delta P_z| \ll |P_z^-|$, the second term in (4.39) becomes important. We set $\dot{P}_z^- = 0$ to get

$$(P_z^-)_{\text{qs}} = -P_c \frac{1}{1 + \varepsilon}, \quad (\delta P_z)_{\text{qs}} = P_c \frac{\varepsilon}{1 + \varepsilon}. \quad (4.43)$$

We have to prove that δP_z takes on its quasi-static value before the system passes the resonance. The solution of (4.39) is given by

$$\delta P_z(t) = \delta P_z(0) \exp\left(-\int_0^t \kappa(t) dt\right). \quad (4.44)$$

If we substitute $x = T(t)/T_{\text{res}}$, we can write the integral as

$$F_-(t) \equiv \int_0^t \kappa dt = \frac{k_D m_{\text{pl}} 2 P_z^+ k_A}{6.3^{1/6} 5.5 k_T^{1/6}} \frac{s^2 |\delta m^2|^{1/6}}{c^{11/6}} I_-(t), \quad (4.45)$$

where

$$I_-(t_{\text{res}}) = \int_1^\infty \frac{x^6(x^6 - 1)}{[k_D^2 x^{12} + (x^6 - 1)^2]^2} dx \approx 293. \quad (4.46)$$

Assuming that initially δP_z and P_z^- are of the same order of magnitude, we know that δP_z will decrease by a factor of order $\varepsilon \sim b_T/b_A \sim \mathcal{O}(10^{-6})$, which corresponds to $F_-(t_{\text{res}}) \geq 6 \ln(10)$. Thus, we obtain the condition

$$s^2 |\delta m^2|^{1/6} \gtrsim 10^{-12} \text{eV}^{1/3} \quad (4.47)$$

using $P_z^+ \approx 1$.

For P_z^+ we can perform a similar calculation. However, here we demand that P_z^+ does *not* change significantly to prevent that the repopulation terms become important. Therefore we demand that $F_+(t_{\text{res}}) \ll 1$, where

$$P_z^+(t) = P_z^+(0) \exp[-F_+(t)]. \quad (4.48)$$

Thus,

$$F_+(t) = \int_0^t \kappa(t)\varepsilon(t)dt = \frac{k_D m_{\text{pl}} k_T^{1/2}}{6.3^{1/2} 5.5} \frac{s^2 |\delta m^2|^{1/2}}{c^{3/2}} I_+(t), \quad (4.49)$$

where

$$I_+(t_{\text{res}}) = \int_1^\infty \frac{x^2}{k_D^2 x^{12} + (x^6 - 1)^2} dx \approx 15.2. \quad (4.50)$$

We then get the condition

$$s^4 |\delta m_{\text{eV}}^2| \ll 2 \times 10^{-9}, \quad (4.51)$$

where $\delta m_{\text{eV}}^2 = \delta m^2 / \text{eV}^2$. $F_+(t_{\text{res}}) \leq 1$ is also the condition that the ν_s do not come into equilibrium. Our result here is in good agreement with previous constraints [48].

The quasi-static approximation is of course not exact, actually the variables will always be a bit behind their quasi-static values. This delay becomes important when the quasi-static value of a variable passes zero, or when the rate of change of the quasi-static value becomes of order of the damping rate of the variable. At resonance, i.e. when $(b_c - b_T) = 0$, we have $\vartheta_{\text{qs}}^- = 0$, $\varphi_{\text{qs}}^+ = 0$, $(P_z^-)_{\text{qs}} = 0$. Furthermore, all the quasi-static values change relatively fast near the resonance.

Here is a qualitative discussion of the behavior of the variables close to resonance. The term that is responsible for the resonance, $\Delta b \equiv b_c - b_T$, only enters into the differential equation of φ^+ . When Δb changes sign, φ_{qs}^+ does too. Therefore, after a short delay, φ^+ will also change its sign. The other variables do not depend directly on Δb ; they only feel its change via φ^+ . Thus, they are not sensitive to the time delay between φ^+ and φ_{qs}^+ . Therefore, setting $\varphi^+ = \varphi_{\text{qs}}^+$ will merely shift the events by a negligible amount of time.

Close to resonance, we have $\sin \varphi^+ \approx 0$ and $\cos \varphi^+ \approx 1$. Therefore, ϑ^+ becomes maximal close to the resonance, i.e. $\vartheta^+ \approx b_s/D$, while ϑ^- becomes minimal so that we can neglect it in the equations. φ^- will stay close to its quasi-static value since δP_z does not change significantly: δP_z freezes out when the rate of change in $(\delta P_z)_{\text{qs}}$ becomes larger than the damping rate κ , i.e. $r_{\delta P_z} > \kappa$, where $r_{\delta P_z}$ is given in (A.7). Since $\Delta b \equiv b_c - b_T \ll D$ and $\varepsilon \ll 1$ at freeze-out, we get

$$r_{\delta P_z} \approx -6H \frac{b_c}{\Delta b}, \quad \kappa \approx \frac{2P_z^+ b_s^2 b_A \Delta b}{D^3}. \quad (4.52)$$

Using $T = T_{\text{res}}$, we find that $\Delta b_{\text{fr}} = -8.1 \times 10^{-9} s^{-1} |\delta m_{\text{eV}}^2|^{-1/12} c^{11/12} b_T$, and thus $\varepsilon_{\text{fr}} = 7.2 \times 10^{-3} s |\delta m_{\text{eV}}^2|^{5/12} c^{-7/12} \ll 1$, so that $(\delta P_z)_{\text{fr}} \approx \varepsilon_{\text{fr}} P_c$ is indeed very small.

In summary, at resonance we can still approximate the variables ϑ^+ , φ^+ and φ^- by their static values, while we can neglect ϑ^- . δP_z is given by its freeze-out value.

4.7 Evolution at Resonance

We now come to the most interesting feature of the system: $\sin \varphi^+$ changes its sign and becomes positive. Therefore, the back-reaction of φ^- on δP_z , which is given by the coefficients of the first terms in (4.24) and (4.28), $b_A \cdot b_s P_z^+ \vartheta^+ \sin \varphi^+$, also changes its sign to positive. So while δP_z until now was washed out through this back-reaction, the same back-reaction now amplifies δP_z . We will now derive the consequences of this effect. To this end, we will assume that the variables ϑ^\pm and φ^\pm will be given approximately by their static values. As time passes, these approximations will break down and we will need to find other approximations.

4.7.1 Static Approximation after Resonance

The change of δP_z becomes interesting again when $r_{\delta P_z} \leq \kappa$ after the resonance, i.e. when $\Delta b_0 = -\Delta b_{\text{fr}}$. We will denote the time when this happens with t_0 . So until then, $\delta P_z(t_0) \approx (\delta P_z)_{\text{fr}} = \varepsilon_{\text{fr}} P_c$. Now (4.39) has changed to

$$\frac{d}{dt} \delta P_z = +\kappa(\delta P_z - \varepsilon P_z^-) \approx +\kappa(\delta P_z + \varepsilon P_c). \quad (4.53)$$

If we neglect the second term, we get the solution

$$\delta P_z(t) = \delta P_z(t_0) \exp\left(\int_{t_0}^t \kappa dt\right). \quad (4.54)$$

To solve the integral, we substitute t with $\xi = 1 - x \ll 1$, where $x = T(t)/T_{\text{res}}$. Then

$$\Delta b = b_c - b_T = b_c^{\text{res}} x^{-1} - b_T^{\text{res}} x^5 = b_T^{\text{res}} x^{-1} (1 - x^6) \approx 6 b_T^{\text{res}} \xi, \quad (4.55)$$

and

$$d\xi = -\frac{1}{T_{\text{res}}}dT = \frac{5.5T_{\text{res}}^2x^3}{m_{\text{pl}}}dt \approx \frac{5.5T_{\text{res}}^2}{m_{\text{pl}}}dt, \quad (4.56)$$

where we have expanded ξ and have only taken into account the leading order. The integral becomes

$$\begin{aligned} \int_{t_0}^t \kappa dt &= \frac{m_{\text{pl}}}{5.5T_{\text{res}}^2} \int_{\xi_0}^{\xi} \kappa d\xi \approx \frac{m_{\text{pl}}}{5.5T_{\text{res}}^2} \int_{\xi_0}^{\xi} \frac{2P_z^+ b_s^2 b_A 6b_T^{\text{res}} \xi}{D^3} d\xi \\ &= \frac{2P_z^+ b_s^2 b_A 6b_T m_{\text{pl}}}{D^3 5.5T^2} \Big|_{T=T_{\text{res}}} \int_{\xi_0}^{\xi} \xi d\xi \\ &= 5.5 \times 10^{17} s^2 |\delta m_{\text{eV}}^2|^{1/6} c^{-11/6} \cdot \frac{1}{2} (\xi^2 - \xi_0^2), \end{aligned} \quad (4.57)$$

where we have assumed that $\Delta b \ll D$ and have again expanded ξ to leading order. Furthermore, $\xi_0 = \Delta b_0 / 6b_T^{\text{res}} = 1.35 \times 10^{-9} s^{-1} |\delta m_{\text{eV}}^2|^{-1/12} c^{11/12}$.

The solution (4.54) is only valid as long as φ^- and ϑ^- can follow their static approximations, which are given by (4.37) and (4.38). We see that as long as $\Delta b = b_c - b_T \ll D$, the changes in φ_{qs}^- and ϑ_{qs}^- will mainly be due to δP_z , i.e. $\dot{\varphi}_{\text{qs}}^- / \varphi_{\text{qs}}^- \approx \dot{\vartheta}_{\text{qs}}^+ / \vartheta_{\text{qs}}^+ \approx \frac{d}{dt} \delta P_z / \delta P_z$. Then the validity of (4.54) breaks down when $D = \frac{d}{dt} \delta P_z / \delta P_z = \kappa$, which happens when $\xi = \xi_1 = 1.1 \times 10^{-14} s^{-2} |\delta m_{\text{eV}}^2|^{1/3} c^{7/3}$. We see that the above solution already breaks down very early, for a large parameter range we even have $\xi_1 < \xi_0$. To give an estimate of how big the integral (4.57) will be, we set $\xi_0 = 0$ and get $\int_{t_{\text{res}}}^{t_1} \kappa dt = 0.8 \times 10^{-11} s^{-2} |\delta m_{\text{eV}}^2|^{5/6} c^{17/6}$, which means that the change in δP_z between t_{res} and t_1 is negligible. So we can immediately give up the static approximations for φ^- and ϑ^- .

4.7.2 Mathematical Pendulum

After the quasi-static approximation for φ^- breaks down, the first term in (4.28) will be the dominant one due to the rapid growth of δP_z , so we neglect the other terms. In (4.24), we can neglect the terms with the slowly varying ϑ^- . Since $b_A \gg b_s \vartheta^+ \sin \varphi^+$, P_z^- will have a much larger effect on $\dot{\varphi}^-$ than on $d(\delta P_z)/dt$, so that soon $\varphi^- \gg P_z^-$, and we can thus neglect the third term in (4.24). Therefore we get the simplified equations

$$\frac{d}{dt} \delta P_z \approx b_s (\vartheta^+ \sin \varphi^+) \sin \varphi^- \quad (4.58)$$

$$\frac{d}{dt}\varphi^- \approx b_A \delta P_z. \quad (4.59)$$

Together, they give the second order equation

$$\ddot{\varphi}^- \approx g \sin \varphi^-, \quad (4.60)$$

where $g = b_A b_s (\vartheta^+ \sin \varphi^+)$. We have now found a very simple description of the system. In the next two subsections, we will discuss the features of this equation. Afterwards, we discuss the consequences for our system.

We take $t = t_0$ to be the initial time. Then the initial conditions are given by

$$\varphi_0^- = \varphi_{\text{qs}}^- \approx \frac{b_A}{D} (\delta P_z)_{\text{fr}} \ll 1, \quad \dot{\varphi}^- \approx 0. \quad (4.61)$$

For definiteness, we take φ_0^- to be positive, which implies $\delta P_z > 0$.

Let us first assume that g is constant. Then the differential equation corresponds to a mathematical pendulum, where g is the acceleration of gravity, see Fig. 4.3. Usually, we could apply the small angle expansion around the stable minimum of the potential energy. However, in our case $\varphi^- = 0$ corresponds to the meta-stable maximum of the potential energy. So our system will perform large-amplitude oscillations. We denote the amplitude of the oscillations with φ_{max}^- , so small φ_{max}^- corresponds to large amplitude. For illustration, we can define the analogy of a potential energy $E_{\text{pot}} = -g(1 - \cos \varphi^-)$ and a kinetic energy $E_{\text{kin}} = \frac{1}{2}(\dot{\varphi}^-)^2$. Conservation of energy implies that the total energy $E_{\text{tot}} = E_{\text{pot}}(t_0) + E_{\text{kin}}(t_0) = \text{const}$. Since $E_{\text{tot}}(t_0) < 0$, we know that the system will oscillate around the stable point $\varphi^- = \pi$ with constant amplitude $\varphi_{\text{max}}^- = |\varphi_0^-|$, and that φ^- will never pass the meta-stable point $\varphi^- = 0$. We can also state that due to the non-linearity of $\sin \varphi^-$, the oscillation frequency of the system, ν , will be smaller than the oscillation frequency $\sqrt{g}/2\pi$ for the linear small-angle approximation. In fact, for $E_{\text{tot}} \rightarrow 0$, the oscillation frequency goes to zero. In Fig. 4.4, we have plotted the ratio $2\pi\nu/\sqrt{g}$ as a function of the amplitude φ_{max}^- .

Another important fact is that the time average of $\cos \varphi^-$, $\langle \cos \varphi^- \rangle$, is greater than 0 for small φ_{max}^- , i.e. for large amplitudes. This results from the fact that the system develops relatively slowly close to the turning points $\pm\varphi_{\text{max}}^-$, where the kinetic energy is small. We have plotted $\langle \cos \varphi^- \rangle$ as a function of the amplitude φ_{max}^- in Fig. 4.5.

Next, we discuss the differential equation with time dependent g . It is sufficient if we deduce the effect on the amplitude φ_{max}^- ; we can then use φ_{max}^- and Figs. 4.4 and 4.5 to derive the oscillation frequency and $\langle \cos \varphi^- \rangle$.

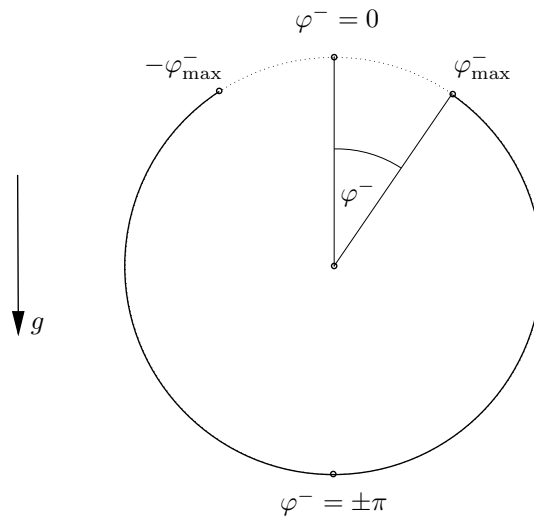


Figure 4.3: Pictorial view of our pendulum.

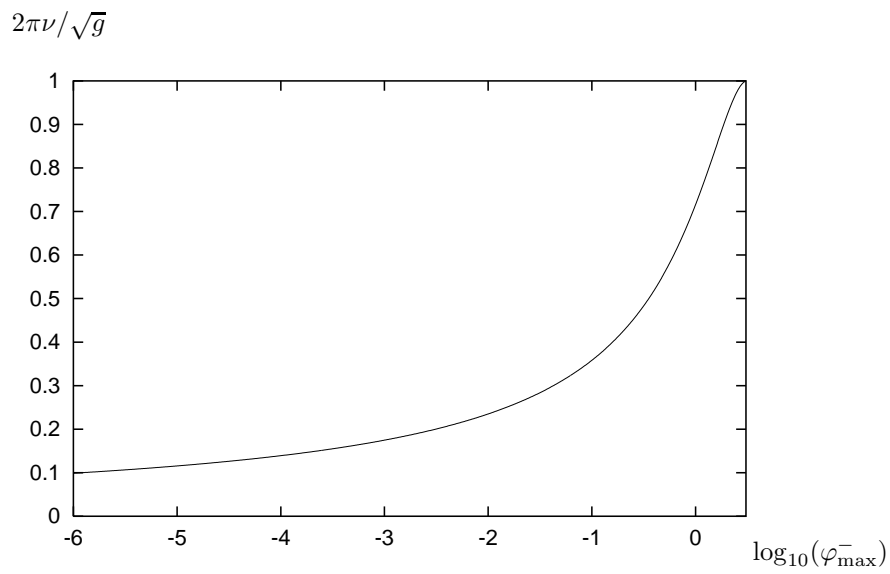


Figure 4.4: Frequency of the pendulum as a function of the amplitude.

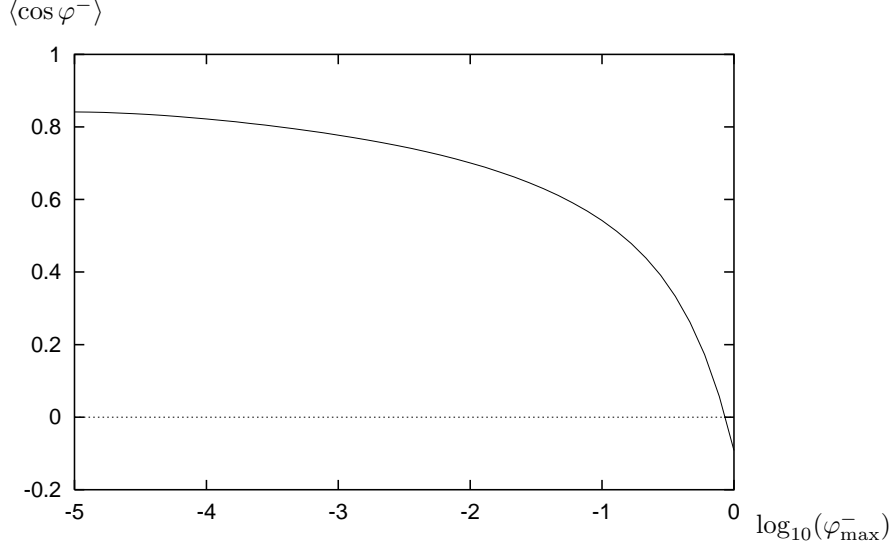


Figure 4.5: The average $\cos \varphi^-$ as a function of the amplitude.

We will assume that \dot{g} is approximately constant over the time of half the oscillation period, $\tau/2$, where $\tau = 1/\nu \geq 2\pi/\sqrt{g}$. Then it is easy to calculate the change in the amplitude $d\varphi^-$ during the time $dt = \tau/2$. Taking the differential of the potential energy, we get

$$dE_{\text{pot}}^{\max} = -dg (1 - \cos \varphi_{\max}^-) + g d(\cos \varphi^-) \quad (4.62)$$

Since the acceleration of gravity, g , is no longer constant, the total energy is not conserved, so that

$$\begin{aligned} \dot{E}_{\text{tot}} &= \dot{E}_{\text{kin}} + \dot{E}_{\text{pot}} = \dot{\varphi}^- \ddot{\varphi}^- - g \sin \varphi^- \dot{\varphi}^- - \dot{g}(1 - \cos \varphi^-) \\ &= -\dot{g}(1 - \cos \varphi^-), \end{aligned} \quad (4.63)$$

where the first two terms cancel due to the differential equation (4.60). We get the differential

$$dE_{\text{tot}} \approx -dg (1 - \langle \cos \varphi^- \rangle), \quad (4.64)$$

where we have time averaged $\cos \varphi^-$. Equating (4.62) and (4.64), we get

$$d(\cos \varphi_{\max}^-) = -\frac{dg}{g} (\cos \varphi_{\max}^- - \langle \cos \varphi^- \rangle), \quad (4.65)$$

If we use $dg = \dot{g} dt = \dot{g} \tau/2$ and $d(\cos |\varphi^-|) = d(\cos |\varphi^-|) = -\sin |\varphi^-| d|\varphi^-|$, we finally get

$$d|\varphi_{\max}^-| = -\frac{\dot{g}\tau/2}{g \sin |\varphi_{\max}^-|} \left(\cos \varphi_{\max}^- - \langle \cos \varphi^- \rangle \right) \quad (4.66)$$

as the change in the amplitude during one half oscillation, where of course $\cos \varphi_{\max}^- \geq \langle \cos \varphi^- \rangle$. We see that $\dot{g} > 0$ will result in a decreasing amplitude, i.e. increasing $|\varphi_{\max}^-|$. Analogously, $\dot{g} < 0$ will result in an increasing amplitude. If thereby $|\varphi_{\max}^-| + d|\varphi_{\max}^-| < 0$, $E_{\text{tot}} > 0$, so the system passes the meta-stable point and accelerates on the other side instead of turning. Then it is better to use (4.64) instead of the differential for the amplitude to describe how the system evolves.

Our approximation breaks down if $|\varphi_{\max}^-| + d|\varphi_{\max}^-| \ll 1$, since then $(\cos \varphi_{\max}^- - \langle \cos \varphi^- \rangle) \rightarrow 0$, $\sin^{-1} \varphi_{\max}^- \rightarrow \infty$ and $\tau \rightarrow \infty$. Also, $\dot{g} = \text{const}$ might not apply any longer.

Now we can already make a statement about the neutrino asymmetry, represented by $\delta P_z = \dot{\varphi}^-/b_A$. If $E_{\text{tot}} < 0$, the asymmetry will change sign at the turning points $\pm \varphi_{\max}^-$, i.e. the asymmetry oscillates. If $E_{\text{tot}} > 0$, the asymmetry will oscillate between $\sqrt{2E_{\text{tot}}}/b_A$ and $\sqrt{2(E_{\text{tot}} + g)}/b_A$, but will not change sign.

4.7.3 The Factor g

The next step is to derive \dot{g} . The factors b_A and b_s in g only vary slowly with time, and we will take them to be constant. Thus the main contribution to \dot{g} comes from $\vartheta^+ \sin \varphi^+$. For convenience, we define two new variables, $\alpha = \vartheta^+ \sin \varphi^+$ and $\beta = \vartheta^+ \cos \varphi^+$. Then $g = b_s b_A \alpha$, so that $\dot{g} \propto \dot{\alpha}$. We get

$$\dot{\alpha} = -D\alpha + (b_c - b_T)\beta \quad (4.67)$$

$$\dot{\beta} = -D\beta - (b_c - b_T)\alpha + b_s \cos \varphi^-, \quad (4.68)$$

where we have neglected all terms dependent on ϑ^- .

Initially, $\varphi^- \ll 1$, so we will first consider the simpler case where $\cos \varphi^- = 1$, $\sin \varphi^- = 0$. Then we can apply the quasi-static approximation for ϑ^+ and φ^+ . Thus,

$$\alpha_{\text{qs}} = \frac{b_s(b_c - b_T)}{D^2 + (b_c - b_T)^2} \quad (4.69)$$

$$\beta_{\text{qs}} = \frac{b_s D}{D^2 + (b_c - b_T)^2}. \quad (4.70)$$

Now we can determine $\dot{g} = b_s b_A \dot{\alpha}_{\text{qs}}$ with the help of

$$\dot{\alpha}_{\text{qs}} = H \frac{b_s(-b_T \Delta b^2 + D^2 \Delta b + D^2 b_c)}{[D^2 + \Delta b^2]^2}, \quad (4.71)$$

where $\Delta b = b_c - b_T$.

For small Δb , $\dot{\alpha}_{\text{qs}}$ is positive. However, $\dot{\alpha}$ changes sign when the numerator becomes zero, i.e.

$$\Delta b_\alpha = \frac{D^2}{2b_T} \left(1 \mp \sqrt{1 + 4 \frac{b_c b_T}{D^2}} \right). \quad (4.72)$$

Using $b_c \approx b_T = D/k_D$, we find that the term $b_c b_T / D^2 \approx k_D^{-2} \gg 1$. Therefore,

$$\Delta b_\alpha \approx D = k_D b_T. \quad (4.73)$$

This result can be expressed in terms of the dimensionless variable $\xi = 1 - T(t)/T$. Then we get $\xi_\alpha \approx k_D/6$, see (4.55).

In summary, g will increase at first and then decrease for $\Delta b > \Delta b_\alpha$. We have plotted the parameter-independent dimensionless variables $\alpha_{\text{qs}} c/s$ and $\frac{d}{d\xi} \alpha_{\text{qs}} c/s = \dot{\alpha}_{\text{qs}} T_{\text{res}} c/HTs$ as a function of ξ in Figs. 4.6 and 4.7, respectively. We can see that $\dot{\alpha}_{\text{qs}}$ is constant to lowest order for very small ξ . Therefore, we expand g in terms of ξ ,

$$g = 6 \frac{b_A b_s^2 b_T}{D^2} \Big|_{T_{\text{res}}} \xi + \mathcal{O}(\xi^2). \quad (4.74)$$

This approximation is valid for $\xi < \xi_\alpha$.

Now we consider the situation where φ^- changes in time. We assume that the oscillation period $\tau = \mathcal{O}(1/\sqrt{g})$ is much smaller than the damping time scales $1/D$ and $1/\Delta b$. Then we can approximate $\sin \varphi^-$ and $\cos \varphi^-$ by their time average values, 0 and $\langle \cos \varphi^- \rangle$, respectively, when describing the evolution of α and β . Thus

$$\dot{\alpha} \approx -D\alpha + \Delta b \beta \quad (4.75)$$

$$\dot{\beta} \approx -D\beta - \Delta b \alpha + b_s \langle \cos \varphi^- \rangle. \quad (4.76)$$

Note that here we can easily neglect ϑ^- , since $\vartheta_{\text{qs}}^- \propto \langle \sin \varphi^- \rangle = 0$. The coefficient Δb in (4.75) and (4.76) induces an oscillation of the two variables, which

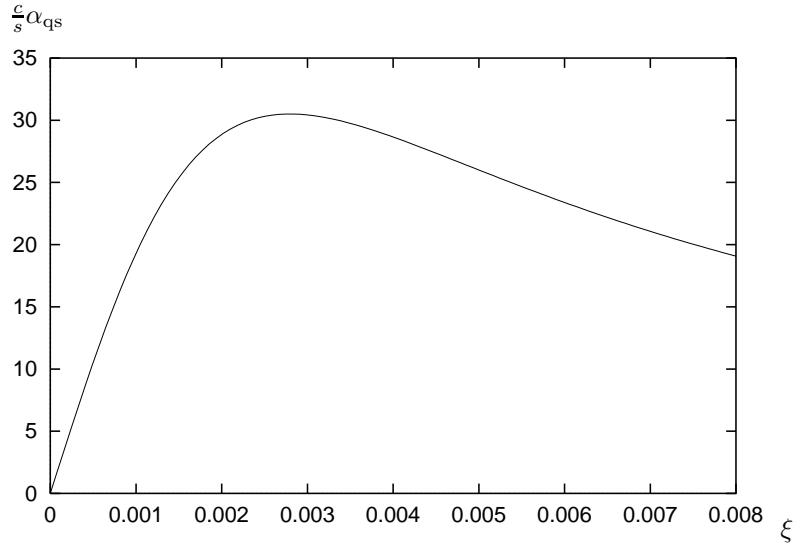


Figure 4.6: Evolution of $\frac{c}{s}\alpha_{qs}$, given in (4.69), as a function of $\xi = 1 - T/T_{res}$.

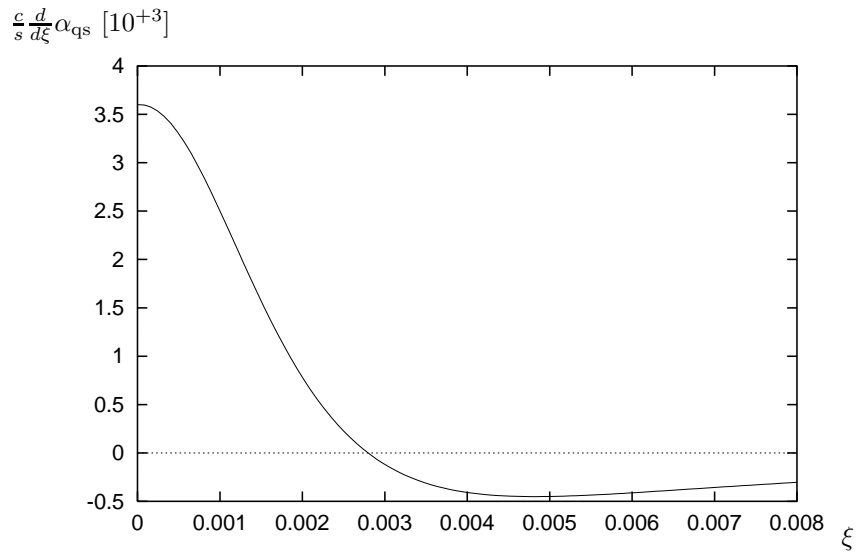


Figure 4.7: Evolution of $\frac{c}{s} \frac{d}{d\xi} \alpha_{qs} = \frac{c T_{res}}{s HT} \dot{\alpha}_{qs}$ as a function of ξ .

will be damped by the coefficient D toward their quasi-static approximations, given by

$$\alpha_{\text{qs}} = \frac{b_s \Delta b}{D^2 + \Delta b^2} \langle \cos \varphi^- \rangle, \quad (4.77)$$

$$\beta_{\text{qs}} = \frac{b_s D}{D^2 + \Delta b^2} \langle \cos \varphi^- \rangle. \quad (4.78)$$

4.7.4 Proof for Oscillations

It is now easy to describe the evolution of our system. We will restrict ourselves to proving that the pendulum, and therefore δP_z , will oscillate for a certain range of mixing parameters. δP_z will change sign at least once if \dot{g} is positive during the first oscillation of φ^- , since then the amplitude φ_{max}^- decreases.

We start with the initial values given in (4.61). For small φ^- , we can linearize the differential equation (4.60), so that

$$\ddot{\varphi}^- \approx g \varphi^-. \quad (4.79)$$

Furthermore, we linearize g as we have done in (4.74) and substitute dt by $d\xi$, as shown in (4.56). Then we get

$$\frac{d^2 \varphi^-}{d\xi^2} = h \xi \varphi^-, \quad (4.80)$$

where $h = 1.02 \times 10^{20} s^2 c^{-4/3} |\delta m_{\text{eV}}^2|^{2/3}$. The solutions for this equation are the Airy-functions.

When $\varphi^- = \mathcal{O}(1)$, the linear approximation breaks down, and φ^- will start oscillating with a frequency $\nu \lesssim \sqrt{g}/2\pi$. We want $\dot{g} \propto \dot{\alpha}$ to be positive, so this first oscillation has to start before ξ_α . Thus we demand $\xi_{\varphi^-} < \xi_\alpha$, where ξ_{φ^-} is defined by $\varphi^-(\xi_{\varphi^-}) = 1$. We find numerically that we can fit the solution of this condition with

$$s^{3.1} |\delta m_{\text{eV}}^2| \geq 10^{-15.1} \quad (4.81)$$

for $|\delta m^2| = 10^{-9} - 10^5 \text{ eV}^2$ with an error smaller than 3%.

Of course, we need to take into account that the quasi-static solution for α given in 4.69 breaks down, since $\langle \varphi^- \rangle < 1$ during oscillations. However, as we can see in (4.75) and (4.76), $\dot{\alpha}$ does not depend on $\langle \cos \varphi^- \rangle$ directly, but

indirectly through $\Delta b\beta$. Thus, the change in $\langle \cos \varphi^- \rangle$ will first affect $\dot{\alpha}$ after a time scale $1/\Delta b$. So if the condition $\Delta b \ll \sqrt{g}$ holds at $\xi = \xi_{\varphi^-}$, then $\dot{\alpha}$ stays positive during the first few oscillation periods, and thus the amplitude will decrease.

Since $\Delta b/\sqrt{g} \propto \sqrt{\xi}$, we can use the stronger condition $\Delta b/\sqrt{g} \ll 1$ for $\xi = \xi_\alpha$. Then we get

$$s|\delta m_{eV}^2|^{-1/6} \gg 3 \times 10^{-6}. \quad (4.82)$$

We have now found the conditions for which δP_z oscillates.

We can also estimate the amplitude with which the neutrino asymmetry δP_z oscillates. An upper bound is given if we use the maximal value for g , i.e. at $\xi = \xi_\alpha$, and assume $E_{\text{tot}} = 0$. Then $\delta P_z = \dot{\varphi}^-/b_A$ is maximal at $\varphi^- = \pi$, i.e. $E_{\text{kin}} = -E_{\text{pot}} = 2g$. We derive

$$\begin{aligned} (\delta P_z)_{\text{max}} &= \frac{1}{b_A}(\dot{\varphi}^-)_{\text{max}} = \frac{1}{b_A}\sqrt{2(E_{\text{kin}})_{\text{max}}} \\ &= \frac{1}{b_A}\sqrt{4g(\xi_\alpha)} \approx \frac{2}{b_A}\sqrt{\frac{b_s^2 b_A}{2D}} \\ &\approx 1.4 \times 10^{-2} s |\delta m_{eV}^2|^{1/6} c^{-5/6}. \end{aligned} \quad (4.83)$$

We can compare this result with the numerical solution given in Section 4.2. Numerically we find during the period where δP_z oscillates that $\delta P_z \leq 7.53 \times 10^{-7}$ for the parameters $\delta m^2 = -1 \text{ eV}^2$, $s = 10^{-4}$. This is in very good agreement with our analytical value $(\delta P_z)_{\text{max}} = 1.4 \times 10^{-6}$. The difference is due to the fact that when g is maximal, the amplitude of φ^- is not maximal, and thus a factor of $\sqrt{2}$ has to be replaced by $\sqrt{1 + \cos \varphi_{\text{max}}^-}$. Furthermore, α is slightly decreased due to $\langle \cos \varphi^- \rangle < 1$.

Chapter 5

Conclusions

We have analytically examined neutrino oscillations between a sterile and an active neutrino in the Early Universe, neglecting the neutrino momentum distribution. Our main achievement has been to prove that this system, which is known to create a large neutrino asymmetry, exhibits oscillations of this neutrino asymmetry for a large range of mixing parameters, as shown in Fig. 5.1. We conclude that these asymmetry oscillations, which have been encountered in only some of the numerical calculations, can not arise from numerical instabilities.

With the methods presented in our work, the complete analytical treatment of this system seems to have become feasible. Naturally, the next step will be to include the effects from the neutrino momentum distribution on the oscillatory behavior. Then the analytical approach will clearly be superior to the numerical one, which continues to encounter many difficulties [49]. Finally, the duration of the asymmetry oscillations and the power law of the asymmetry growth after the oscillations have ceased should be derived.

Understanding the mechanism of ν_α - ν_s oscillations in the Early Universe is very important. On the one hand, if the primordial abundances are determined with sufficient precision, it becomes possible to constrain the mixing parameters of the ν_α - ν_s system. As a result, some of the models which have been proposed to explain the current experimental situation could be excluded.

On the other hand, if future neutrino experiments, such as MiniBooNE [42], prove the existence of a sterile neutrino, it is necessary to understand the impact of the ν_s on the primordial abundances to test whether BBN is a consistent theory.

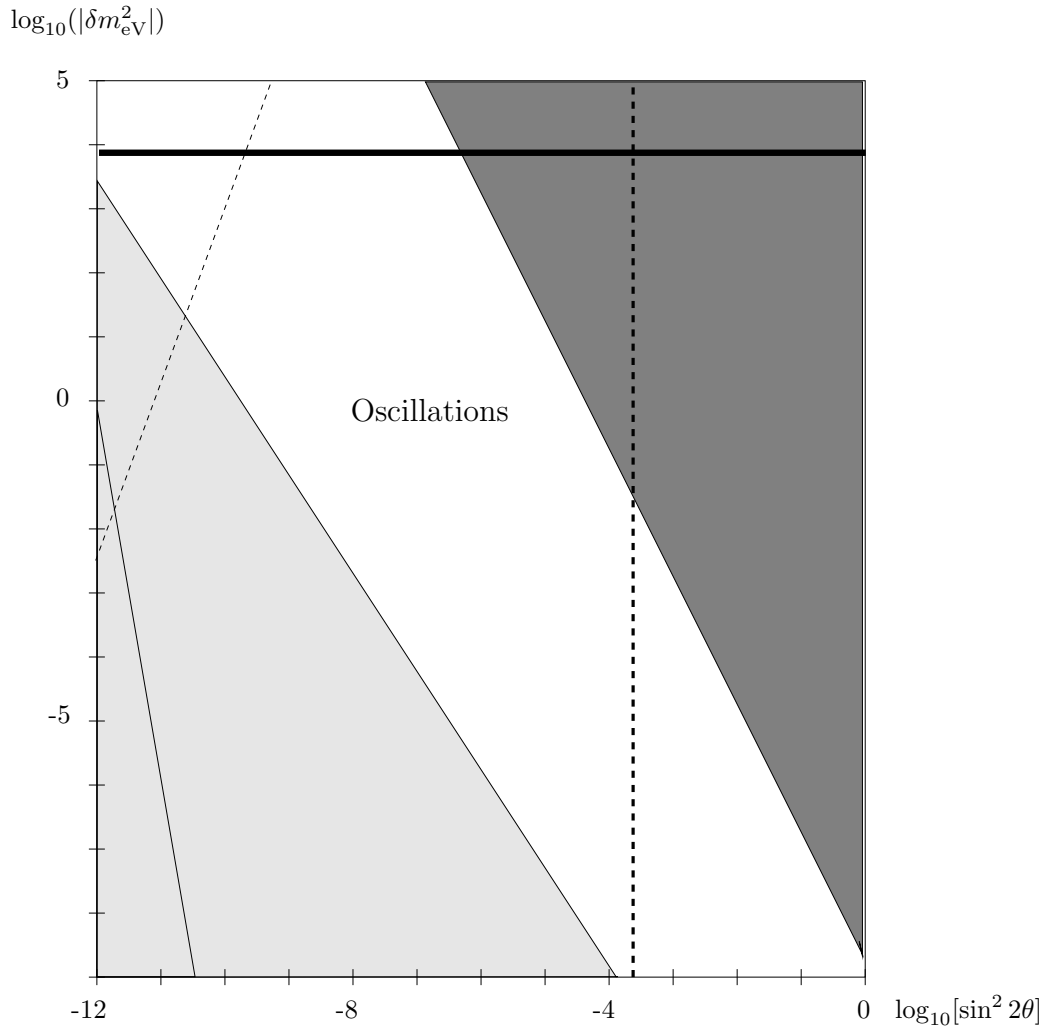


Figure 5.1: Bounds on the parameter space derived in our work. In the central white region, our proof of asymmetry oscillations is valid. In the dark-shaded region, the sterile neutrinos come into equilibrium, see (4.51). In the light-shaded region, the factor g starts decreasing again before $\varphi^- = \mathcal{O}(1)$, see (4.81); we cannot say whether the asymmetry oscillates in this region of parameter space. Below the lower left line, δP_z does not reach its quasi-static solution before resonance, see (4.47). Our small-angle approximation, $s \ll k_D$, is valid only to the left of the thick dashed line. To the left of the thin dashed line, the condition (4.82) does not apply; still, there might be oscillations. Above the horizontal thick line, the universe would be over-closed [8].

Appendix A

Quasi-Static Approximation and its Range of Validity

The quasi-static approximation of a variable x which follows the differential equation

$$\frac{\partial}{\partial t}x(t) = -D(t)x(t) + f(t) \quad (\text{A.1})$$

is given by

$$x_{\text{qs}} = \frac{f}{D}. \quad (\text{A.2})$$

If f and D depend on time, x_{qs} also changes its value. Therefore, x_{qs} will only be a good approximation if the quasi-static condition is fulfilled, i.e.

$$|\dot{x}_{\text{qs}}| < Dx_{\text{qs}}. \quad (\text{A.3})$$

We have derived all values $r_x \equiv \dot{x}_{\text{qs}}/x_{\text{qs}}$ for our system of differential equations (4.23)–(4.28) assuming that all variables except for P_z^+ are at their static values, where $H = -\dot{T}/T$.

$$r_{\vartheta^+} \equiv \frac{\dot{\vartheta}_{\text{qs}}^+}{\vartheta_{\text{qs}}^+} = -6H \left(-1 + \frac{b_c(b_c - b_T)}{D^2 + (b_c - b_T)^2} \right), \quad (\text{A.4})$$

$$r_{\varphi^+} \equiv \frac{\dot{\varphi}_{\text{qs}}^+}{\sin \varphi_{\text{qs}}^+} = -6H \frac{-b_c}{b_c - b_T} \frac{D}{\sqrt{D^2 + (b_c - b_T)^2}}. \quad (\text{A.5})$$

Here we have divided by $\sin \varphi_{\text{qs}}^+$ instead of φ_{qs}^+ , since the differential equation for φ^+ has the form $\frac{\partial}{\partial t}x(t) = -D(t) \sin[x(t)] + f(t)$. In the case of φ^- , we

can neglect the sin as long as $\varphi^- \ll 1$. Furthermore,

$$r_{P_z^-} \equiv \frac{(\dot{P}_z^-)_{\text{qs}}}{(P_z^-)_{\text{qs}}} = -\frac{\dot{\varepsilon}}{\varepsilon} \frac{1}{1+\varepsilon}, \quad (\text{A.6})$$

$$r_{\delta P_z} \equiv \frac{\frac{d}{dt}(\delta P_z)_{\text{qs}}}{(\delta P_z)_{\text{qs}}} = \frac{\dot{\varepsilon}}{\varepsilon} \frac{1}{1+\varepsilon}, \quad (\text{A.7})$$

$$\begin{aligned} r_{\vartheta^-} &\equiv \frac{\dot{\vartheta}_{\text{qs}}^-}{\vartheta_{\text{qs}}^-} = r_{\vartheta^+} + r_{P_z^-} \\ &= -H \left(-8 - 6 \frac{b_c}{b_c - b_T} \left(1 - 3 \frac{(b_c - b_T)^2}{D^2 + (b_c - b_T)^2} \right) \right) + r_{\delta P_z}, \end{aligned} \quad (\text{A.8})$$

$$\begin{aligned} r_{\varphi^-} &\equiv \frac{\dot{\varphi}_{\text{qs}}^-}{\varphi_{\text{qs}}^-} = -6H \frac{b_c}{b_c - b_T} + r_{P_z^-} \\ &= -H \left(-2 + 12 \frac{b_c(b_c - b_T)}{D^2 + (b_c - b_T)^2} \right) + r_{\delta P_z}, \end{aligned} \quad (\text{A.9})$$

where

$$\varepsilon = -\frac{D^2 + (b_c - b_T)^2}{2P_z^+ b_A (b_c - b_T)}, \quad (\text{A.10})$$

$$\frac{\dot{\varepsilon}}{\varepsilon} = -H \left(2 + 6 \frac{b_c}{b_c - b_T} \left(1 - 2 \frac{(b_c - b_T)^2}{D^2 + (b_c - b_T)^2} \right) \right). \quad (\text{A.11})$$

Bibliography

- [1] B.T. Cleveland et al. Nucl. Phys. B (Proc. Suppl.) **38**, 47 (1995); K.S. Hirata et al., Phys. Rev. **D44**, 2241 (1991); GALLEX Collaboration, Phys. Lett. **B388**, 384 (1996); J.N. Abdurashitov et al., Phys. Rev. Lett. **77**, 4708 (1996).
- [2] Y. Fukuda, *et al.*, Phys. Rev. Lett. **81**, 1562 (1998); Y. Fukuda, *et al.*, Phys. Lett. **B433**, 9 (1998); Y. Fukuda, *et al.*, Phys. Lett. **B436**, 33 (1998).
- [3] C. Athanassopoulos et al. Phys. Rev. Lett. **75** (1995) 2650; C. Athanassopoulos et al. Phys. Rev. **C58** (1998) 2489.
- [4] B. Pontecorvo, Zh. Eksp. Teor. Fiz. **33**, 549 (1957)/ Sov. Phys. JETP **7**,172 (1958).
- [5] With kind permission from G. Raffelt, to be published in *Proceedings 1998 Summer School in High-Energy Physics and Cosmology, ICTP*, hep-ph/9902271.
- [6] Particle Data Group, *Review of Particle Physics*, European Physical Journal **C3** (1998), 1.
- [7] H. Nunokawa, J.T. Peltoniemi, A. Rossi, J.W.F. Valle, Phys. Rev. **D56**, 1704 (1997).
- [8] E.W. Kolb, M.S. Turner, *The Early Universe*, Addison-Wesley (1990).
- [9] K. Enqvist, K. Kainulainen, J. Maalampi, Phys. Lett. **B244**, 186 (1990); Phys. Lett. **B249**, 531 (1990); Nucl. Phys **B349**, 754 (1991); R. Barbieri, A. Dolgov, Phys. Lett. **B237**, 440 (1990).
- [10] R. Barbieri, A. Dolgov, Nucl. Phys. **B349**, 743 (1991).

- [11] R. Foot, M.J. Thomson, R.R. Volkas, Phys. Rev. **D53**, 5349 (1996).
- [12] R. Foot, R.R. Volkas, Phys. Rev. Lett. **75**, 4350 (1995).
- [13] R. Foot, R.R. Volkas, Phys. Rev. **D55**, 5147 (1997).
- [14] X. Shi, G.M. Fuller, Phys. Rev. **D59**, 063006 (1999).
- [15] R. Foot, Astropart. Phys. **10**, 253 (1999).
- [16] R. Foot, R.R. Volkas, astro-ph/9811067.
- [17] X. Shi, G.M. Fuller, astro-ph/9812232.
- [18] R. Foot, R.R. Volkas, Phys. Rev. **D59**, 029901 (1999).
- [19] N.F. Bell, R. Foot, R.R. Volkas, Phys. Rev. **D58**, 105010 (1999).
- [20] R. Foot, R.R. Volkas, hep-ph/9904336.
- [21] X. Shi, Phys. Rev. **D54**, 2753 (1996).
- [22] K. Enqvist, K. Kainulainen, A. Sorri, hep-ph/9906452.
- [23] X. Shi, G.M. Fuller, Phys. Rev. Lett. (to be published), astro-ph/9904041.
- [24] A.D. Dolgov, S.H. Hansen, S. Pastor, D.V. Semikoz, hep-ph/9910444.
- [25] P. Di Bari, hep-ph/9911214.
- [26] X. Shi, G.M. Fuller, K. Abazajian, astro-ph/9904052.
- [27] P. Di Bari, P. Lipari, M. Lusignoli, hep-ph/9907548.
- [28] N.F. Bell, R.R. Volkas, Y.Y.Y. Wong, Phys. Rev. **D59**, 113001 (1999).
- [29] X. Shi, G.M. Fuller, K. Abazajian, Phys. Rev. **D60**, 063002 (1999).
- [30] R. Foot, hep-ph/9906311.
- [31] M.V. Chizhov, D.P. Kirilova, hep-ph/9908525.
- [32] R. Foot, R.R. Volkas, Astropart. Phys. **7**, 283 (1997).

- [33] X. Shi, G.M. Fuller, K. Abazajian, astro-ph/9908081.
- [34] X. Shi, G.M. Fuller, Phys. Rev. Lett. **82**, 2832 (1999).
- [35] K. Abazajian, X. Shi, G.M. Fuller, astro-ph/9909320.
- [36] M.V. Chizhov, D.P. Kirilova, hep-ph/9909408.
- [37] K. A. Olive, D.N. Schramm, D. Thomas, T.P. Walker, Phys. Lett. **B265**, 239 (1991).
- [38] B.D. Fields, K.A. Olive, Ap.J. **506**, 177 (1998).
- [39] S. Burles, D. Tytler, Ap.J. **499**, 699 (1998);
S. Burles, D. Tytler, Ap.J. **507**, 732 (1998).
- [40] J.K. Webb, R.F. Carswell, K.M. Lanzetta, R. Ferlet, M. Lemoine, A. Vidal-Madjar, D.V. Bowen, Nature **388**, 250 (1997);
D. Tytler, S. Burles, L. Lu, X.-M. Fan, A. Wolfe, B.D. Savage, astro-ph/9810217, to appear in Astron.J..
- [41] K.A. Olive, G. Steigman, T.P. Walker, astro-ph/9905320.
- [42] A.O. Bazarko, hep-ex/9906003.
- [43] C.W. Kim, A. Pevsner, Neutrinos in Physics and Astrophysics, Harwood Academic Publishers (1993).
- [44] G.G. Raffelt, Stars as Laboratories for Fundamental Physics, The University of Chicago Press (1996).
- [45] D. Nötzold, G. Raffelt, Nucl. Phys. **B307**, 924 (1988).
- [46] B.H.J. McKellar, M.J. Thomson, Phys Ref. **D49**, 2710 (1994).
- [47] L. Stodolsky, Phys. Rev. **D36**, 2273 (1987).
- [48] X. Shi, D.N. Schramm, B.D. Fields, Phys. Rev. **D48**, 2563 (1993).
- [49] P. Di Bari, R. Foot, hep-ph/9912215.